Since January 2020 Elsevier has created a COVID-19 resource centre with free information in English and Mandarin on the novel coronavirus COVID-19. The COVID-19 resource centre is hosted on Elsevier Connect, the company's public news and information website.

Nonneoplastic Disorders of the Brain

William B. Thomas

Computed tomography (CT) and magnetic resonance imaging (MRI) are helpful in the diagnosis of many nonneoplastic brain disorders in the dog and cat. The ability of CT and MRI to depict normal and abnormal anatomy facilitates the identification of developmental anomalies, including hydrocephalus, Chiari malformations, arachnoid cysts, and cerebellar hypoplasia. These imaging modalities also allow the detection of hemorrhage and infarction and are therefore useful in the evaluation of spontaneous cerebrovascular disorders and head trauma. Finally, many inflammatory diseases, such as encephalitis, brain abscess, and parasite migration, cause abnormalities detectable by CT and MRI. Although more research on the imaging features of specific nonneoplastic brain disorders is needed, current information indicates that CT and MRI are useful in the management of these disorders.

Recent advances in imaging techniques have greatly improved the ability to detect pathologic processes in the brain, localize lesions precisely, and predict the type of disease more accurately than ever before.[1] Although most reports of computed tomography (CT) and magnetic resonance imaging (MRI) of brain disease in veterinary medicine have focused on the diagnosis of brain tumors, these imaging methods are also valuable in the evaluation of various nonneoplastic brain diseases. The purpose of this article is to provide an overview for imaging some of the more frequently encountered nonneoplastic diseases of the brain. Clinical features of each disease are included because imaging can supplement but never replace a careful history and thorough physical and neurological examination. Typical pathological changes are also mentioned, because CT and MRI reflect gross and microscopic pathology and an understanding of the expected pathological changes can be very helpful in predicting imaging findings. Ideally, a review article such as this would be based on systematic research and clinical data. Unfortunately, the current literature on imaging of nonneoplastic brain disease in veterinary patients is fairly sparse. Therefore, the information presented in this article is based on the limited data regarding veterinary patients supplemented by the much more complete information on comparable diseases in human patients, as well as my own experience. As more information becomes available, the conclusions in this article may have to be modified.

From the Department of Small Animal Clinical Sciences, College of Veterinary Medicine, University of Tennessee, Knoxville, TN.

Address reprint requests to William B. Thomas, DVM, MS, Diplomate ACVIM (Neurology), Department of Small Animal Clinical Sciences, University of Tennessee, PO Box 1071, Knoxville, TN 37901-1071.

1096-2867/99/1403-0002$10 00/0

Technical Considerations

Imaging strategies for CT and MRI are similar to those described for intracranial neoplasia. (Refer to the article entitled "Intracranial Neoplasia" by Kraft and Gavin in the May 1999 issue.) Throughout this chapter, the MRI features of the various disorders are those depicted with spin echo imaging. Readers should refer to the article entitled "Advanced Imaging Concepts: A Pictorial Glossary of CT and MRI Technology" by Tidwell and Jones in the May 1999 issue for a description of other pertinent MRI techniques such as gradient echo and inversion recovery pulse sequences, magnetic resonance angiography, and diffusion/perfusion imaging.

Disorders

Disorders of Brain Development

Hydrocephalus

Hydrocephalus is a pathological condition in which there is accumulation of cerebrospinal fluid (CSF) within the cranium.[2,3] This usually occurs within the ventricular system (internal hydrocephalus) but can involve the subarachnoid space (external hydrocephalus).[3] Hydrocephalus is not a specific disease, but rather a multifactorial disorder with a variety of pathophysiological mechanisms. CSF is produced at a constant rate by the choroid plexuses of the lateral, third, and fourth ventricles; the ependymal lining of the ventricular system; and blood vessels in the subarachnoid space. The CSF circulates through the ventricular system into the subarachnoid space, where it is absorbed by arachnoid villi.[3] Hydrocephalus can be caused by a blockage of the flow of CSF, called obstructive hydrocephalus, or secondary to decreased volume of brain parenchyma, termed hydrocephalus ex vacuo. (Increased formation of CSF is virtually never a cause of hydrocephalus.) A number of conditions, such as infarction and necrosis, can result in decreased volume of brain parenchyma and hydrocephalus ex vacuo. Obstruction to CSF flow can occur anywhere along the pathway from its formation to the site of absorption in the cranial and spinal arachnoid villi. Obstruction within the ventricular system or at its outflow through the lateral apertures is called noncommunicating hydrocephalus because the ventricular system does not communicate with the subarachnoid space. Obstruction within the subarachnoid space or at the level of absorption in the arachnoid villi is called communicating hydrocephalus.[2]

Hydrocephalus can be classified further as congenital or acquired. Congenital hydrocephalus is most common in toy-breed dogs. The causes are diverse and include genetic factors, developmental anomalies, and intrauterine or perinatal infection or bleeding in the brain. Congenital hydrocephalus may be associated with a wide range of other nervous system anomalies, including meningomyelocele, Chiari malformation,

Dandy-Walker syndrome, and cerebellar hypoplasia. Clinical signs of congenital hydrocephalus include an enlarged, dome-shaped head with persistent fontanelles and open cranial sutures. Neurological deficits include abnormal behavior, disturbed consciousness, ataxia, circling, blindness, seizures, and vestibular dysfunction. In mature dogs, diseases such as tumors and inflammatory diseases can cause acquired hydrocephalus. Neurological deficits are similar to those in puppies, but if hydrocephalus develops after the cranial sutures have closed, malformation of the skull does not develop.[2,3]

CT and MRI allow accurate assessment of ventricular size, extent of cortical atrophy, and the presence of any focal lesions that may account for the hydrocephalus. Imaging is also useful in monitoring patients after surgical placement of ventriculoperitoneal shunts used for treatment. Changes in ventricular size can be monitored, and the presence of complications such as subdural hematoma or hygroma can be evaluated.[4]

Ventricular size is usually assessed subjectively, noting the progressively greater proportion of the intracranial volume occupied by the lateral, third, and/or fourth ventricles[4,5] (Fig 1). Several investigators have provided quantitative measurements. When measured at the level of or caudal to the interthalamic adhesion, Hudson et al[6] state that lateral ventricles are considered enlarged if lateral ventricular height exceeds 0.35 cm or the ratio between the height of the lateral ventricle and the width of the cerebral hemisphere (ventricle-hemisphere ratio) exceeds 0.19. Spaulding and Sharp[7] consider the lateral ventricles enlarged if the ratio between lateral ventricular height and the dorsoventral height of the cerebral hemisphere exceeds 0.14. However, there is a poor correlation between clinical signs and ventricular size, and symmetric or asymmetric enlargement of the lateral ventricles is relatively common in normal adult dogs and puppies.[6-10] Therefore, diagnosis of hydrocephalus must be based on clinical features, not just ventricular size.

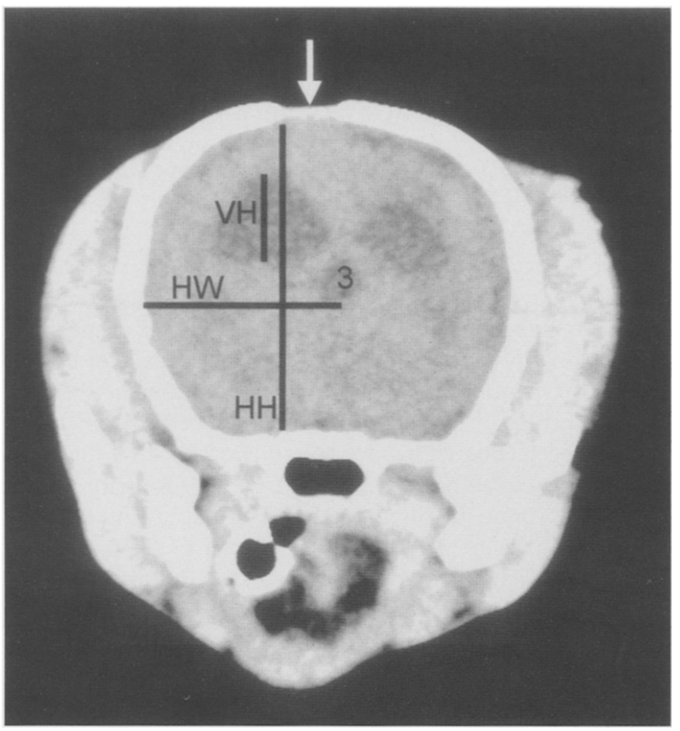

Fig 1. Transverse noncontrast CT image of a dog with hydrocephalus. There is asymmetric enlargement of the lateral ventricles, enlargement of the third ventricle (3) and a persistent bregmatic fontanelle (arrow). Several measurements used in the quantification of ventriculomegaly are shown: VH, ventricular height; HH, hemisphere height; HW, hemisphere width.

Hydrocephalus ex vacuo can be distinguished from obstructive hydrocephalus based on enlarged cortical sulci and subarachnoid space secondary to atrophy of brain parenchyma (Fig 2). In obstructive hydrocephalus, the site of obstruction may be identified by dilatation of CSF spaces proximal to the obstruction, and normal or collapsed spaces distally. For example, obstruction at the level of the third ventricle would be expected to result in enlarged lateral ventricles but no enlargement of the mesencephalic aqueduct and fourth ventricle (Fig 3). Dilatation of all the ventricles and the subarachnoid space implies an obstruction at or near the arachnoid villi. Unfortunately, this simplistic approach has limited accuracy. For example, 25% to 35% of human patients with communicating hydrocephalus have little or no dilatation of the fourth ventricle.[4] Obstructing masses, such as tumors, granulomas, and cysts, may be identified, especially on postcontrast images (Fig 3). MRI is more sensitive than CT in showing small focal lesions, especially those in the caudal fossa.[4]

Periventricular edema may be identified in some patients with hydrocephalus. Experimentally, acute obstructive hydrocephalus in dogs causes edema starting at the dorsolateral angles of the lateral ventricles and spreading into the adjacent white matter.[11] On CT, this is evident as blurring or loss of the normally sharp ventricular margins.[4] The edema is best appreciated on T2-weighted MRI as increased intensity compared with normal white matter.[11] Periventricular edema is most frequently associated with acute hydrocephalus and increased intraventricular pressure, rather than chronic, relatively compensated hydrocephalus with normal intraventricular pressure.[4]

Imaging techniques make it possible to readily identify ventriculomegaly but may give little clue as to its clinical significance. It is therefore necessary to interpret the finding of ventriculomegaly in context with clinical features.

Chiari Malformations

Chiari described four unrelated types of malformations of the brainstem and cerebellum in human patients. The most common is Chiari I malformation, which consists of caudal displacement of a portion of the cerebellum through the foramen magnum into the cervical portion of the vertebral canal. The cause is an underdeveloped occipital bone that induces overcrowding of the caudal fossa, which is accommodated by caudal displacement of the cerebellum.[12]

Many human patients with this malformation develop hydromyelia (a dilatation of the central canal of the spinal cord that is lined by ependyma) and/or syringomyelia (an accumulation of fluid within the spinal cord that is not lined by ependyma). The term syringohydromyelia is often used because it can be difficult or impossible to tell whether the cavity is lined with ependyma except at necropsy. Syringohydromyelia in Chiari I malformation is caused by obstruction of CSF flow at the foramen magnum. The brain expands as it fills with blood during systole, inducing a pressure wave in the CSF that is accommodated in normal subjects by rapid movement of CSF from within the skull to the vertebral canal. With obstruction to rapid movement of CSF through the foramen magnum, the caudal portion of the cerebellum moves down-

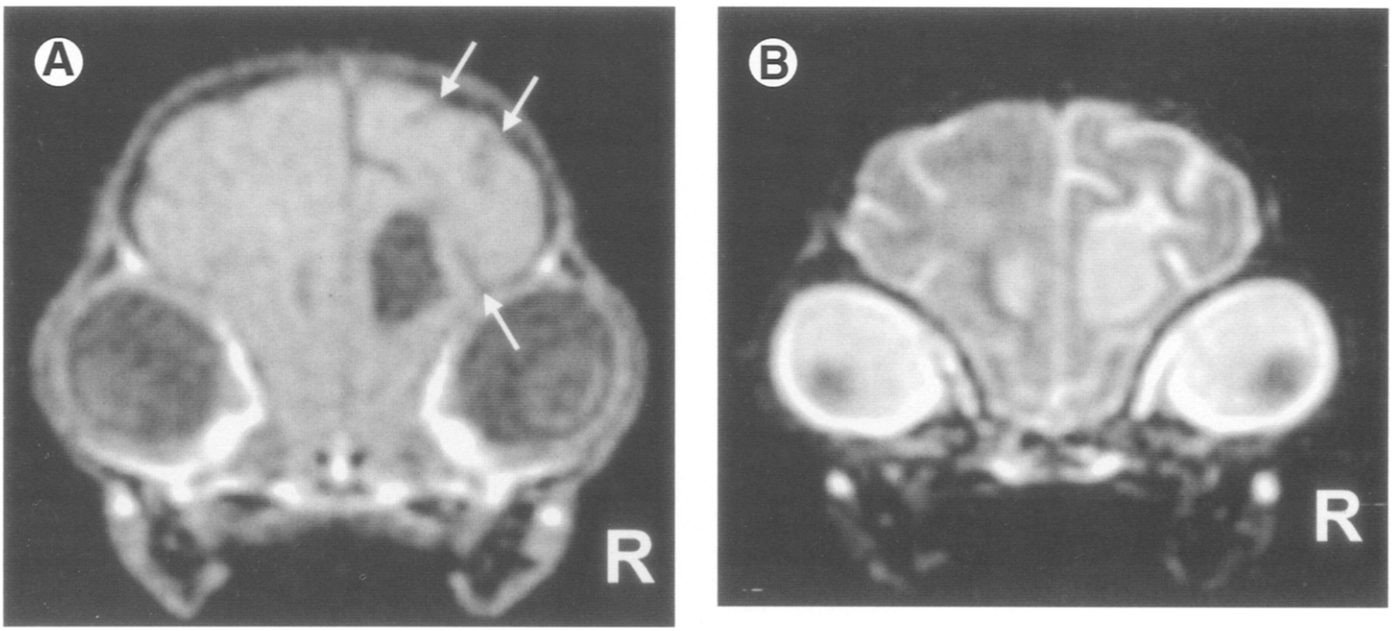

Fig 2. Hydrocephalus ex vacuo secondary to necrotizing encephalitis in a Yorkshire terrier. (A) On the transverse T1-weighted MR image, enlargement of the rostral aspect of the right lateral ventricle is evident. There is loss of parenchymal volume of the right frontal lobe evident as increased prominence of the adjacent sulci (arrows) compared with the left. SE, 600/20, 0.5 T. (B) Transverse T2-weighted image shows the enlarged hyperintense CSF-filled sulci of the right frontal lobe. SE, 3000/100, 0.5 T. (Reprinted with permission.[115])

ward with each systolic pulse, acting as a piston on the surface of the spinal cord. This relentless compression of the spinal cord propels CSF into and within the syrinx.[13] Some patients also have hydrocephalus attributed to obstruction of CSF flow in the crowded caudal fossa. Clinical signs of Chiari I malformation in human beings can develop in childhood or adulthood and include head and neck pain, myelopathy, or encephalopathy.[12,13]

A similar malformation has been reported in adult dogs with neck pain and tetraparesis.[14,15] Diagnosis is best made on sagittal MRI of the craniocervical junction (Fig 4). The caudal portion of the cerebellum is displaced into the vertebral canal to a variable degree.[14,16] The cerebellomedullary cistern is small or absent and the caudal fossa may appear subjectively overcrowded. Hydrocephalus and syringohydromyelia may be evident.[14-16] Syringohydromyelia often involves the caudal cervical or cranial thoracic segments, so this entire region should be imaged. All patients with syringohydromyelia should have imaging of the craniocervical region to rule out a Chiari I malformation or other obstruction of CSF flow.[16]

Chiari II malformation, also known as Arnold-Chiari or Cleland-Chari malformation, involves caudal displacement of the brainstem and cerebellum through an enlarged foramen magnum. The fourth ventricle is elongated and extends caudal to the foramen magnum, and the brainstem may be kinked.[16] Chiari III malformation is displacement of the cerebellum through a cervical spina bifida resulting in a cervical encephalocele. Chiari II and III malformations are not well described in small animals. Chiari IV malformation is severe cerebellar hypoplasia and is discussed separately.[17]

Dandy-Walker Malformations

In human patients, the Dandy-Walker complex is a group of malformations consisting of an enlarged caudal fossa, hypoplasia of the cerebellar vermis, and cystic dilatation of the fourth ventricle that nearly fills the caudal fossa. The cerebellar hemispheres are usually hypoplastic as well. Other anomalies are also common, including hydrocephalus, hypoplasia of the corpus callosum, and syringohydromyelia. Dandy-Walker malformation is caused by outflow obstruction of the fourth ventricle in the developing embryo. This causes dilatation of the fourth ventricle, which enlarges upward between the developing cerebellar hemispheres, preventing their fusion. When the cerebellar hemispheres do not fuse, the vermis does not form.[16]

Analogous malformations have been described in the dog and cat.[14,18-21] In contrast to human patients, most dogs and cats with this syndrome do not have obvious enlargement of the caudal fossa.[18-21] Neurological deficits typically occur at a young age and primarily reflect cerebellar dysfunction, including ataxia, hypermetria, intention tremor, and vestibular dysfunction.[18-21] On CT and MRI, Dandy-Walker malformation is characterized by an enlarged caudal fossa filled by an enormous fourth ventricle and a small cerebellum.[14,16,20,21] The cerebellar vermis may be absent, producing a cleft in the middle of the cerebellum. Hydrocephalus may also be evident.[20,21]

Cerebellar Hypoplasia

A variety of in utero insults and heritable defects may cause failure of normal development of the cerebellum, resulting in a hypoplastic or absent cerebellum. The most common cause in cats is in utero or perinatal infection with the feline panleukopenia virus. Cerebellar hypoplasia has also been reported in dogs, in which a heritable basis has been suspected in some cases, but in utero infections cannot be excluded.[22,23] Single or multiple animals within a litter may be affected. There is nonprogressive ataxia, hypermetria, and intention tremor, first apparent at about the time the animal begins to walk. CT or MRI shows a small or absent cerebellum. The remainder of the

Fig 3. Obstructive hydrocephalus in a dog. (A) On the transverse postcontrast T1-weighted MR image, enlargement of the lateral ventricles and a heterogeneously enhancing mass in the region of the third ventricle are present. (B) Transverse image at the level of the mesencephalon shows a normal-sized aqueduct (arrow). (C) Transverse image at the level of the medulla shows a normal-sized fourth ventricle (arrow). SE, 400/20, 0.5 T.

caudal fossa is filled with CSF. Other anomalies, such as hydrocephalus, may also be apparent.[22]

Arachnoid Cysts

Arachnoid cysts (also called intra-arachnoid cysts) are accumulations of fluid surrounded by a membrane resembling the arachnoid mater. They can develop in the subarachnoid space anywhere along the neuraxis. Congenital arachnoid cysts are developmental anomalies originating from a splitting or duplication of the arachnoid mater. The cyst wall is formed by several layers of arachnoid cells. Acquired arachnoid cysts may result from postinflammatory loculation of CSF caused by trauma, infection, or hemorrhage.[24]

In human beings, congenital intracranial arachnoid cysts may be asymptomatic or cause neurological deficits as the cyst progressively enlarges and compresses adjacent neural structures or interferes with CSF circulation. Enlargement of arachnoid cysts occurs because of fluid production by the cyst wall or an anatomical communication functioning as a one-way valve between the cyst and the subarachnoid space.[24]

Intracranial arachnoid cysts have been reported in the dog and cat.[25,26] The most common location is the subarachnoid space between the cerebellum and the tentorium cerebelli. Clinical signs may occur in immature or mature animals and include seizures, paresis, abnormal behavior, and cranial nerve deficits. In some patients, the cyst is an incidental finding on imaging.[26] On CT, the cyst has well-defined margins and contains fluid that is isodense with CSF (Fig 5). There is

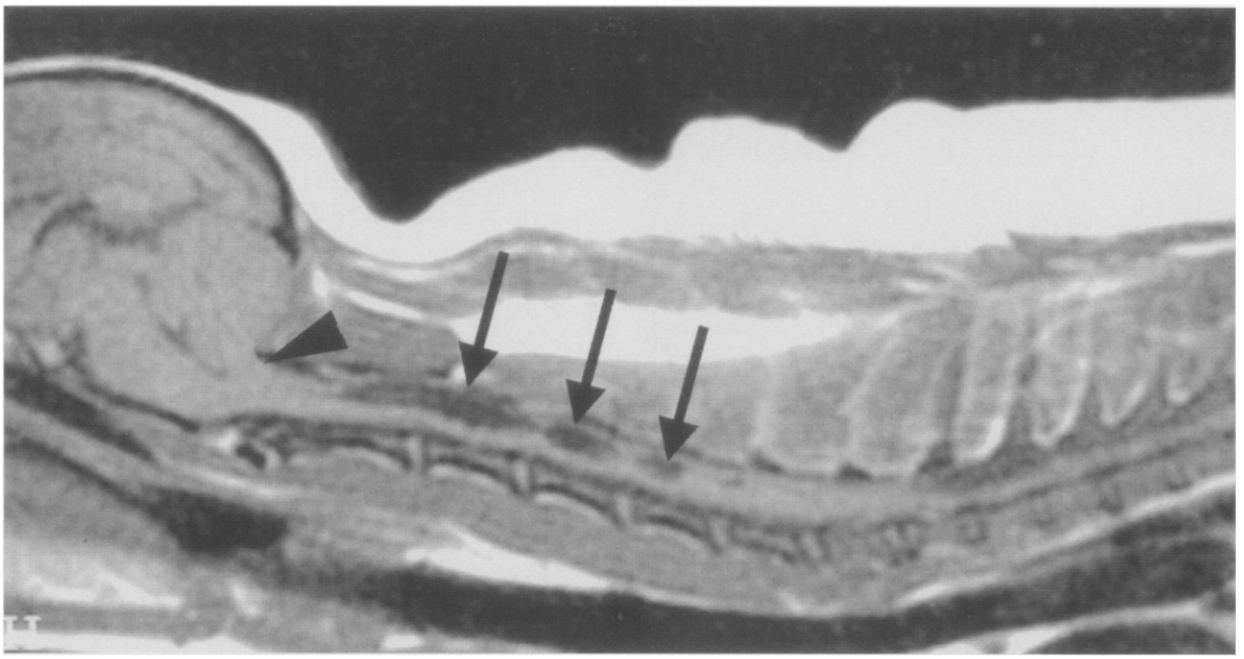

Fig 4. Sagittal noncontrast T1-weighted MR image a dog with Chiari I malformation. There is herniation of the caudal aspect of the cerebellum through the foramen magnum (arrowhead) and syringohydromyelia involving the cervical segments of the spinal cord (arrows). SE, 400/20, 0.5 T.

associated mass effect with no abnormal contrast enhancement.[26] On MRI, these cysts are extra-axial lesions containing fluid with intensity similar to CSF on all image sequences.[25,26] Adjacent neural parenchyma is compressed but of normal intensity, and there is no abnormal enhancement. Obstructive hydrocephalus may develop if the cyst compresses CSF pathways.[26]

Intraparenchymal Hemorrhage

Intracranial hemorrhage can be classified on the basis of location as epidural, subdural, subarachnoid, intraparenchymal, or intraventricular. Epidural, subdural, and subarachnoid hemorrhages are often associated with trauma and are discussed later. Intraparenchymal hemorrhage can be primary or secondary and can extend into the ventricular system. The cause of primary intraparenchymal hemorrhage is incompletely understood. People with this disorder often have systemic hypertension and fibrinoid degeneration of arteries in the brain.[27] Although intracranial hemorrhage caused by hypertension is poorly documented in dogs and cats, primary hypertension and hypertension secondary to other disorders, such as renal disease, hyperadrenocorticism, and hyperthyroidism, are well recognized.[28] These animals may be predisposed to cerebrovascular disease and intracranial hemorrhage.[28] Secondary causes of intracranial hemorrhage include trauma, infarction, congenital vascular malformations, intracranial tumor, vasculitis, and coagulopathies.[29-38] The clinical signs of intraparenchymal hemorrhage consist of a sudden onset of neurological deficits referable to a focal brain lesion. Signs may progressively worsen as the hematoma expands, compressing adjacent neural structures and increasing intracranial pressure.[30-33,36-39]

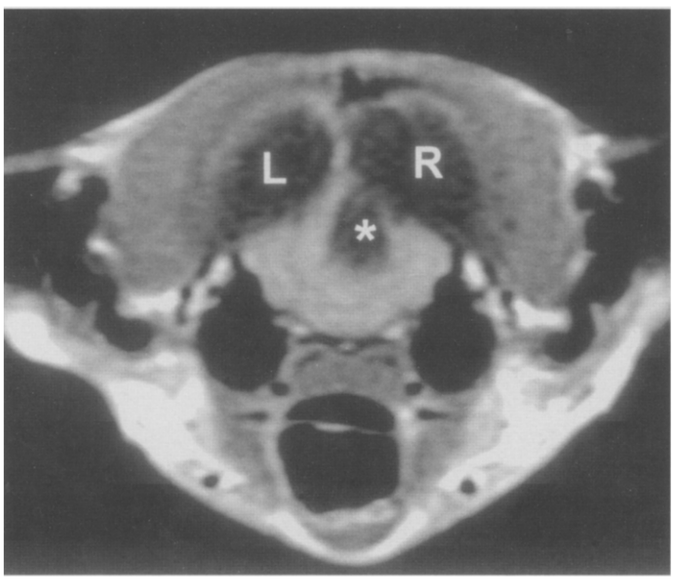

Fig 5. Transverse postcontrast T1-weighted MR image of a cat with an arachnoid cyst. The cyst (asterisk) is present in the dorsal aspect of the cerebellum. Its intensity is the same as CSF, and there is no enhancement. The caudal aspects of the left ventricle (L) and right ventricle (R) are enlarged, secondary to obstruction to CSF flow by the cyst. SE, 600/20, 0.5 T.

Computed Tomography

CT is exquisitely sensitive to acute hemorrhage. Because the attenuation of x-rays is primarily attributable to the globin portion of blood, there is a linear relationship between CT attenuation and hematocrit.[40] The attenuation of whole blood with a hematocrit of 46% is approximately 56 Hounsfield units (HU). In comparison, normal gray matter has an attenuation of 37 to 41 HU, and normal white matter, 20 to 34 HU.[40] Acute hemorrhage in a patient with a normal hematocrit is therefore immediately evident as increased attenuation on CT (Fig 6).[31,36] Hemorrhage in patients with severe anemia may be less obvious. An acute hematoma may be surrounded by a hypodense region corresponding to edema, and there is often an associated mass effect.[31,36,41]

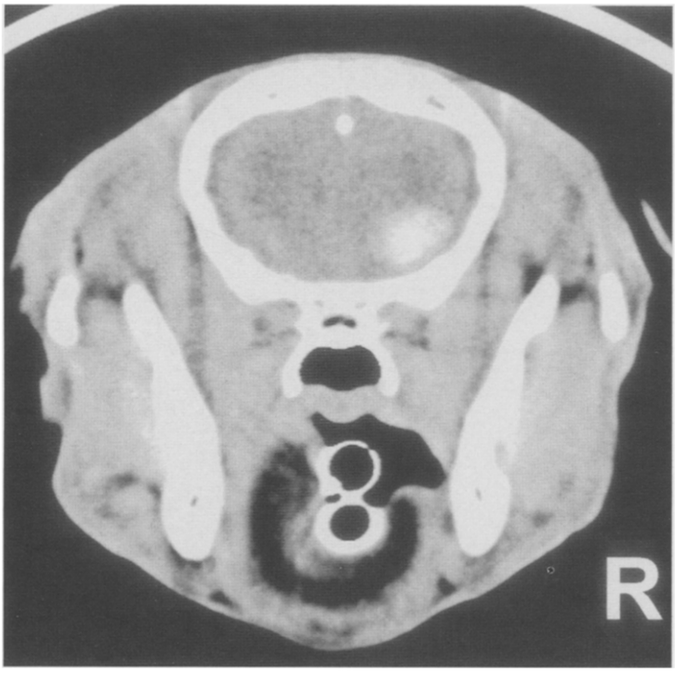

Fig 6. Transverse noncontrast CT image of a dog with intraparenchymal hemorrhage 48 hours after a sudden onset of seizures. A hyperdense lesion consistent with acute hemorrhage is present within the ventral aspect of the right temporal lobe. The lesion is surrounded by hypodense edema. At necropsy, an arteriovenous malformation with hemorrhage was identified.

The attenuation of extravasated blood increases for the first 72 hours with clot formation and extrusion of low-density serum and subsequent increase in hemoglobin concentration.[40] After that, the attenuation gradually decreases as the result of lysis and phagocytosis of erythrocytes, which starts at the periphery and progresses centrally.[40,41] The hematoma eventually becomes isodense at about 1 month after onset.[40,41]

Use of contrast agent is unnecessary in most acute hematomas and may obscure the inherent hyperdensity, confusing the diagnosis. However, use of contrast agent may be helpful if there is a small hemorrhage with mass effect out of proportion to the size of the hematoma. In this instance, the differential diagnosis includes bleeding into a tumor, and contrast may be necessary to visualize the tumor.[40] In hematomas not associated with underlying neoplasia, enhancement first appears at the periphery of the hematoma at approximately 4 to 6 days because of neovascularization.[36,40-42] A ring pattern of enhancement may persist for 2 to 6 weeks.[40]

Magnetic Resonance Imaging

Although variations can occur, the MRI features of most intracranial hematomas follow a predictable course over time. Factors intrinsic to the lesion that affect images include the age of the hemorrhage, whether the bleeding is arterial or venous, the location of the bleeding, and the presence of any underlying lesions. Operator-dependent factors that affect the images include the main magnetic field strength, the exact pulse sequence parameters used, and the method of echo formation.[43]

Hemorrhage can be thought of as an iron salvage pathway, in which iron from the extravasated erythrocytes is mobilized from hemoglobin and converted to short-term iron-containing proteins for transfer to the reticuloendothelial system, or to long-term storage proteins for local deposition.[44] During this process, oxyhemoglobin is converted in a stepwise fashion to deoxyhemoglobin, methemoglobin, and finally ferritin and hemosiderin. These various forms of hemoglobin affect the appearance of hemorrhage in three ways: (1) protein effects that are present with all forms of hemoglobin; (2) paramagnetic relaxation caused by paramagnetic molecules, which is significant only with methemoglobin; and (3) inhomogeneous susceptibility effects induced by paramagnetic forms of hemoglobin (deoxyhemoglobin and methemoglobin) within erythrocytes.[45,46]

Protein effects. Relaxation times are shortened in the presence of proteins in water solutions.[45] This is caused by the changing magnetic fields of nearby nuclei as the molecules undergo Brownian motion.[45] Protein effects are generally proportional to protein concentrations and result in shortening of T1 and T2; that is, increased intensity on T1-weighted images and decreased intensity on T2-weighted images, compared with pure water.[45]

Paramagnetic effects. Biological substances containing unpaired electrons have magnetic properties dominated by the magnetic effects of these unpaired electrons. The magnetic fields of the unpaired electrons are normally oriented randomly such that there is no net magnetization. However, when an external magnetic field is applied, the unpaired electrons tend to align parallel to that field, resulting in enhancement (increased magnitude) of that applied field. Substances that have no intrinsic magnetic field in the absence of an applied magnetic field, but align with and thus enhance that applied field, are termed paramagnetic.[46] Some forms of hemoglobin contain iron with paramagnetic properties, which greatly affects the MRI appearance.

If water molecules approach a paramagnetic center, there is an interaction between the nuclear magnetic dipoles of the water (protons) and the magnetic dipoles of the paramagnetic center (unpaired electrons). This proton-electron dipole-dipole interaction shortens relaxation time of the water protons. For proton relaxation enhancement to occur, however, the water proton must come within about 0.3 nm of the paramagnetic ions' unpaired electrons, because the magnitude of this interaction is inversely proportional to the sixth power of the distance between the dipoles.[46] These paramagnetic effects are more prominent on T1-weighted images than on T2-weighted images.[43] They will therefore result in an increased signal on T1-weighted images, similar to the effects of gadolinium-based contrast agents. (Paramagnetism of MRI contrast medium is also discussed in the Tidwell & Jones article in the May 1999 issue.)

Inhomogeneous susceptibility effects. When paramagnetism is confined to a small region (such as within erythrocytes), there is an inhomogeneous distribution of paramagnetic susceptibility that creates microscopic field gradients.[45] Water molecules diffusing across the erythrocyte membrane experience a fluctuating magnetic field that results in dephasing and shortened T2 relaxation, a process called inhomogeneous susceptibility effect. In spin-echo sequences, inhomogeneous susceptibility effects result in signal loss because of shortened T2 relaxation. This leads to decreased intensity on T2-weighted images.[46]

Hematoma evolution. These three relaxation mechanisms along with proton density contribute to image contrast during the various stages of hematoma formation (Table 1). Because numerous factors can effect the appearance of intracranial hemorrhage on MRI, the following summary is necessarily oversimplified but generally applicable to spin-echo sequences at 0.5 to 2.0 T. (Refer to the Tidwell & Jones article in the May 1999 issue for a discussion on gradient echo imaging of hemorrhage.) Furthermore, the timing of various stages may vary significantly, and different stages often overlap.[43,45] The precise dating of specific hematomas is notoriously inaccurate, so the nomenclature of the temporal stages of hematomas is somewhat arbitrary.[43]

Oxyhemoglobin. Freshly extravasated blood from arterial bleeding is composed of intact erythrocytes containing primarily oxyhemoglobin.[43] The iron in oxyhemoglobin is in the ferrous form (Fe^{+2}). Because there are no unpaired electrons in the iron (or other atoms), oxygenated blood is not paramagnetic.[43] In the absence of paramagnetism, peracute hematomas appear as a high-proton-density region, with slightly shortened relaxation times, compared with water, mainly because of the protein content of blood.[43] This peracute stage of a hematoma usually persists for fewer than 24 hours. Because of their transient nature, peracute hematomas are rarely seen in clinical practice. They are isointense to slightly hypointense on T1-weighted images and hyperintense on T2-weighted images, and therefore appear similar to many other brain lesions.[43,47] Thus, CT is the preferred imaging modality if peracute hemorrhage is suspected.

Deoxyhemoglobin. After a few hours, the oxygen tension within the hematoma is reduced, resulting in the formation of deoxyhemoglobin (acute hematoma). Deoxygenation is usually complete by 24 hours.[45] Removal of molecular oxygen changes the distribution of electrons in the ferrous ion, leaving four unpaired electrons in the outer shell. These unpaired electrons confer deoxyhemoglobin with paramagnetic properties. The paramagnetic iron of deoxyhemoglobin is contained within a hydrophobic crevice in the hemoglobin molecule. This prevents water from coming close enough to the paramagnetic ion to induce paramagnetic (dipole-dipole) interaction. Thus, the hematoma is still isointense to slightly hypointense on T1-weighted images.[43]

As long as the erythrocyte membrane is intact, the paramagnetic deoxyhemoglobin is localized within the cell. This results in inhomogeneous susceptibility effects.[43] Acute hematomas that contain intracellular deoxyhemoglobin consequently appear very hypointense on T2-weighted images.[43] At this stage, any surrounding edema appears as a hyperintense perimeter on T2-weighted images.[43]

Intracellular methemoglobin. As oxygen tension within the hematoma falls further, deoxyhemoglobin is oxidized to methemoglobin (subacute hematoma). In whole blood, methemoglobin begins to accumulate at the rate of about 10% per day, after the first 2 days.[45] Conversion to methemoglobin is maximal when the Po_2 is approximately 20 mm Hg. If the oxygen tension is higher or lower, conversion to methemoglobin is slowed, affecting MRI contrast.[46] The iron in methemoglobin is in the ferric (Fe^{+3}) state, which has five unpaired electrons in its outer shell and is highly paramagnetic. Also, one of the coordination sites of the methemoglobin molecule is occupied by a water molecule that is rapidly exchanged with other water molecules in solution. As a result, water is positioned within 0.3 nm of the paramagnetic iron. This allows paramagnetic (dipole-dipole) interaction to shorten T1 relaxation, causing methemoglobin to be hyperintense on T1-weighted images. This hyperintensity begins at the periphery of an intraparenchymal hematoma and progresses inward, probably because the outer rim of the hematoma has the optimal oxygen tension for the oxidation of hemoglobin.[43,45] At this stage the hematoma is still hypointense on T2-weighted images.[43] Other causes of T1 hyperintensity or T2 hypointensity include fat, calcification, mucinous material, intratumoral melanin, flow effects, and enhancement with paramagnetic contrast agents.[43]

Extracellular methemoglobin. Soon after methemoglobin formation begins, glucose reserves in the erythrocytes are depleted and hemolysis ensues. This eliminates the inhomogeneous susceptibility effect as the methemoglobin becomes uniformly distributed. This prolongs T2, and the hematoma is once again hyperintense on T2-weighted images (rebound hyperintensity).[45] On the other hand, T1-weighted images are not affected and therefore continue to show hyperintensity.[45] This paradoxical state of T1 and T2 hyperintensity may persist for 1 month or more (Fig 7).[45]

Ferritin and hemosiderin. After 2 to 6 weeks, modified macrophages (gitter cells) infiltrate from surrounding brain and remove iron from the hematoma (chronic hematoma). This eventually eliminates the remaining protein and inhomogeneous susceptibility effects. The center of the hematoma eventually either collapses or is replaced by CSF.[45]

The iron is deposited at the periphery of the hematoma as hemosiderin and ferritin, which behave paramagnetically.[43] The iron in these storage forms is not accessible to water, so paramagnetic (dipole-dipole) interaction does not occur, but the inhomogeneous susceptibility effect shortens T2. A chronic hematoma has a rim that is hypointense on T1-weighted images and very hypointense on T2-weighted images. The rim becomes thicker as the hematoma resolves.[45,46] A hypointense

TABLE 1. Spin Echo MRI Appearance of Intracranial Hemorrhage at Medium Field Strength (0.5 T)

Stage	Approximate Time	Magnetic Property	Location of Iron	T1-Weighted Intensity*	T2-Weighted Intensity*
Oxyhemoglobin	First few hours	Diamagnetic	Intracellular	Slightly hypointense	Hyperintense
Deoxyhemoglobin	Several hours to several days	Paramagnetic	Intracellular	Slightly hypointense	Very hypointense
Intracellular methemoglobin	First several days	Paramagnetic	Intracellular	Very hyperintense	Very hypointense
Hemolysis	Several days to several months	Paramagnetic	Extracellular	Very hyperintense	Very hyperintense
Ferritin and hemosiderin	Several days to indefinitely				
Center		Diamagnetic	None	Hypointense	Hyperintense
Rim		Paramagnetic	Extracellular	Hypointense	Very hypointense

*Signal intensities are relative to normal gray matter.
Table compiled from two references [45,138]

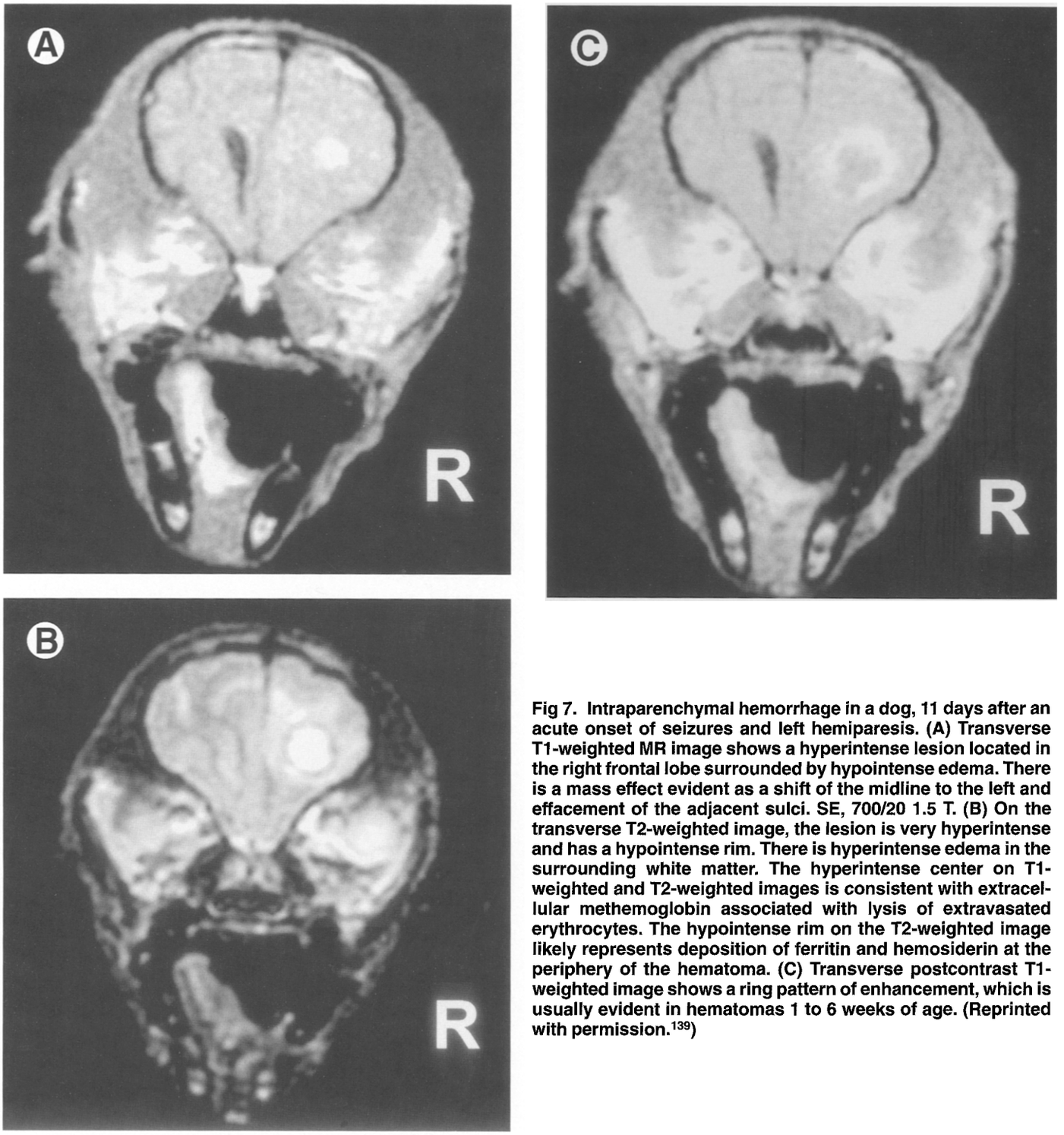

Fig 7. Intraparenchymal hemorrhage in a dog, 11 days after an acute onset of seizures and left hemiparesis. (A) Transverse T1-weighted MR image shows a hyperintense lesion located in the right frontal lobe surrounded by hypointense edema. There is a mass effect evident as a shift of the midline to the left and effacement of the adjacent sulci. SE, 700/20 1.5 T. (B) On the transverse T2-weighted image, the lesion is very hyperintense and has a hypointense rim. There is hyperintense edema in the surrounding white matter. The hyperintense center on T1-weighted and T2-weighted images is consistent with extracellular methemoglobin associated with lysis of extravasated erythrocytes. The hypointense rim on the T2-weighted image likely represents deposition of ferritin and hemosiderin at the periphery of the hematoma. (C) Transverse postcontrast T1-weighted image shows a ring pattern of enhancement, which is usually evident in hematomas 1 to 6 weeks of age. (Reprinted with permission.[139])

region on T2-weighted images can remain indefinitely at the site of an old hematoma.[46]

Differentiating Between Neoplastic and Nonneoplastic Hemorrhage

Whenever intracranial hemorrhage is identified, it is important to determine if it is associated with an underlying tumor or is caused by a nonneoplastic lesion. The use of a contrast agent often allows identification of an underlying tumor.[40] An important finding in a hemorrhagic tumor is persistent surrounding edema (decreased attenuation on CT, hyperintensity on T2-weighted images), whereas edema has usually resolved by the chronic stage of a nonneoplastic hematoma.[43] In neoplastic hemorrhage, MRI signal intensity patterns are more heterogeneous and the temporal evolution of intensity patterns is often delayed compared with nonneoplastic hematomas, probably because hypoxia within the tumor delays methemoglobin formation.[40,43] Neoplastic hemorrhage often lacks the well-defined hypointense rim characteristic of nonneoplastic hematomas in their subacute and chronic stage.[40,43] This is because the persistently altered blood-brain barrier of tumors may allow more efficient removal of ferritin and hemosiderin.[43]

In situations in which the diagnosis is still uncertain, repeat scanning is often useful because this allows evaluation of the expected temporal changes.[40]

Cerebrovascular Malformations

Cerebrovascular malformations result from abnormal development of the vascular network of the brain.[48,49] These lesions are considered congenital and are distinct from vascular neoplasms.[48] Based on morphological and clinical features, cerebrovascular malformations are classified into four major types: arteriovenous, venous, cavernous, and capillary.[48] Arteriovenous malformations are clusters of abnormal arteries and veins with direct arterial-to-venous shunts. Venous malformations are anomalous veins separated by normal neural parenchyma. Cavernous malformations are masses of contiguous sinusoidal vessels with no intervening parenchyma. Capillary malformations, also called telangiectasias, are masses of small, capillary-type vessels separated by normal parenchyma.[48]

Cerebrovascular malformations have been reported in dogs and cats.[29,31-33] The most common is the arteriovenous malformation (*AVM*). Clinical signs are caused by spontaneous hemorrhage and are usually suggestive of a focal cerebral lesion. The onset of signs is usually acute and occurs in middle-aged to older animals.[31-33] The relatively late onset of signs associated with a congenital lesion can be explained by continued hemodynamic stress and consequent attenuation of the abnormal vessels, which eventually leads to hemorrhage.[50]

When a cerebrovascular malformation has bled, early CT or MRI usually shows intraparenchymal hemorrhage (Fig 6).[30-32 37] Contrast-enhanced CT of an *AVM* may show enhancing serpentine vessels. Larger vessels are usually draining veins, smaller ones are feeding arteries.[51] On MRI, the high-flow vascular channels of an AVM may be seen as a cluster of well-defined regions of signal loss (flow voids) on all pulse sequences, although certain MRI sequences can result in high intensity of slowly flowing blood.[51,52] ***Venous malformations*** appear on noncontrast CT as areas of faint, punctate or linear hyperdensity.[51,52] With contrast administration, CT and MRI usually reveal contrast-enhanced curvilinear vascular channels draining a spoke-wheel arrangement of small tapering veins.[51,52] CT of ***capillary malformations*** is often normal, but may show an isodense to slightly hyperdense mass. Contrast enhancement is usually minimal.[51] MRI is more sensitive, and shows a lace-like region of stippled contrast enhancement with no or subtle abnormality on unenhanced images.[52] A ***cavernous malformation*** appears on CT as a focal hyperdense region with variable calcification with mild contrast enhancement.[51 52] On MRI, a cavernous malformation is seen as a central region of mixed intensity, corresponding to methemoglobin, surrounded by circumferential rings of hypointense hemosiderin and ferritin.[52 53]

Whenever a spontaneous intraparenchymal hematoma is identified, it is important to look for any associated large vessels to suggest a vascular malformation. However, the failure to identify large vessels does not entirely exclude a vascular malformation, because compression or obliteration of vessels by adjacent hematoma, extremely slow flow, and thrombosis may obscure the abnormal vessels.[51,52] Although CT and MRI are useful in detecting hemorrhage associated with vascular malformations and depicting the vascular anatomy of some of these lesions, catheter angiography or magnetic resonance angiography (MRA) is often necessary for complete assessment of cerebrovascular malformations in human patients.[51,52,54] (Refer to the Tidwell & Jones article in the May 1999 issue for a discussion of MRA.)

Infarction

Obstruction of flow in the vessels of the brain can result in a sudden onset of neurological signs caused by infarction. Arterial obstruction can be caused by thrombosis or embolism. A thrombus is a blood clot developing within a vessel that causes obstruction at the site of formation. Embolism is occlusion of a vessel by a fragment of blood clot or other substance that has flowed to the site of obstruction from a distant location. Because of abundant venous anastomoses, venous infarction is less common than arterial thromboembolism.[55] In human patients, cerebrovascular thrombosis or embolism is often secondary to atherosclerosis.[56] Atherosclerosis also occurs in dogs, especially older dogs, dogs with hypothyroidism, and miniature Schnauzers with idiopathic hyperlipoproteinemia.[29,57,58] Atherosclerosis associated with these conditions can lead to cerebral thromboembolism and neurological dysfunction.[33 57-59] Other diseases associated with cerebral thromboembolism in dogs include sepsis, coagulopathy, neoplasia, and heartworm infection.[33,60]

Clinical Features

The hallmark of brain infarction is an acute onset of focal brain dysfunction. Neurological deficits depend on the site of the lesion and are typically asymmetric. Involvement of the forebrain, such as with thromboembolism of the middle cerebral artery, usually results in contralateral hemiparesis with decreased postural reactions. Seizures are very common in dogs and cats with infarction affecting the forebrain. There may be contralateral blindness with normal pupillary light reflexes, and the patient may circle or turn toward the side of the lesion. Lesions in the cerebellum may cause ataxia, hypermetria, vestibular dysfunction, or opisthotonos. Brainstem involvement is characterized by gait deficits ranging from ipsilateral hemiparesis to tetraplegia, cranial nerve deficits, and abnormal levels of consciousness, including coma.[30,31,33,36,38,55,61]

Nonhemorrhagic Infarction

Computed tomography. Changes may be detected on CT as early as 3 to 6 hours after onset of signs and consist of a slight decrease in attenuation and subtle mass effect.[62 63] These changes are related to edema and reach a maximum at 3 to 5 days (Fig 8) and resolve by 2 to 3 weeks after infarction.[62] The location and shape of the lesion correspond with the distribution of the involved vessel(s), most commonly the middle cerebral artery.[62] Abnormal contrast enhancement may be seen as early as 24 hours but often does not become evident until about 1 week after infarction.[62,63] Enhancement is most apparent at the periphery of the lesion and reflects growth of new capillaries without a normal blood-brain barrier.[62] Enhancement of hypodense infarcts can result in isodense lesions, thereby masking their presence.[62] For this reason, unenhanced as well as enhanced CT should be performed. In the chronic phase (3 to 4 weeks), the hypodense region becomes more sharply marginated as necrotic tissue is resorbed.[62] Ultimately there is a loss of parenchymal volume with attendant dilatation

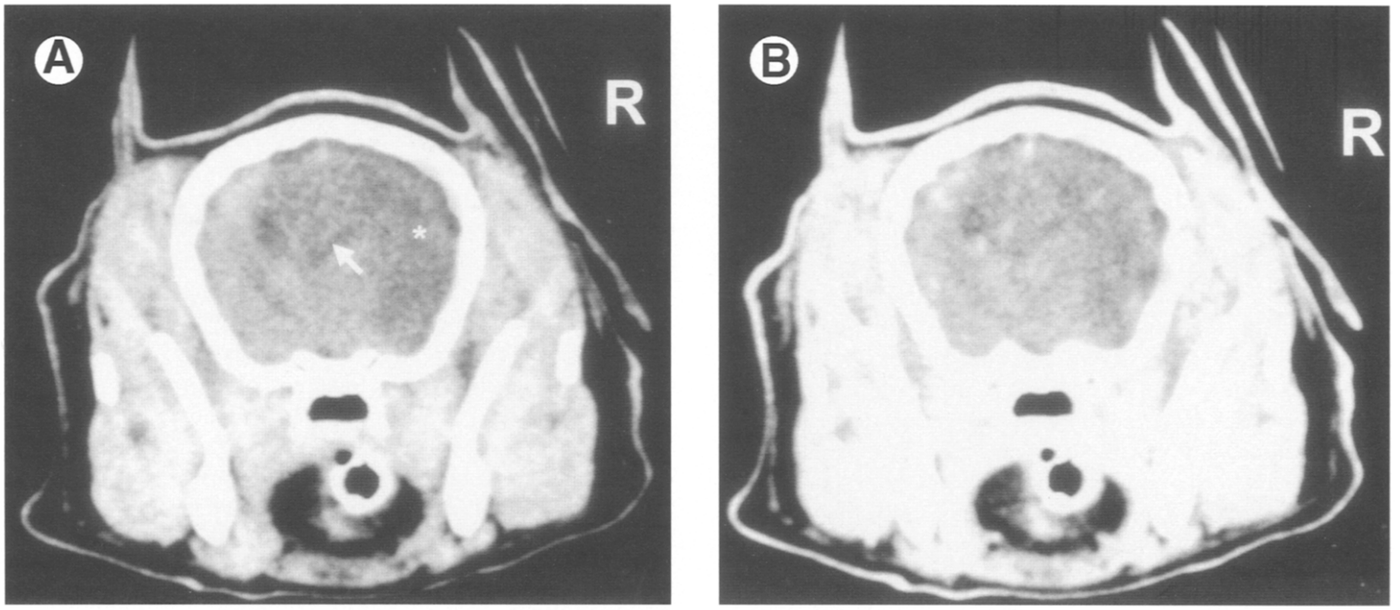

Fig 8. Brain infarct in a dog 4 days after acute onset of focal neurological deficits. (A) Transverse noncontrast CT image shows decreased attenuation of the portion of the brain supplied by the right middle cerebral artery (asterisk). There is substantial mass effect evident as a shift of the midline to the left and displacement of the right lateral ventricle (arrow). (B) Postcontrast image at the same level shows mild, patchy enhancement. Necropsy confirmed infarction in the territory of the right middle cerebral artery. (Courtesy of Karen Inzana, DVM, PhD, Virginia-Maryland Regional College of Veterinary Medicine.)

of adjacent sulci and ventricles.[62] Contrast enhancement does not usually occur in the chronic stage because the integrity of the blood-brain barrier is restored.[62]

Magnetic resonance imaging. Early changes on MRI consist of a subtle increase in intensity on T2-weighted and proton density–weighted images. These changes reflect edema and can be detected as early as 1 hour after vascular occlusion.[64] MRI is thus more sensitive than CT in early infarction. Also, MRI is more sensitive in detecting small infarcts and those involving the brainstem.[65] In acute infarction, T1-weighted MRI is less sensitive than T2-weighed and proton density–weighted images and may be normal.[66] Parenchymal enhancement with gadolinium is uncommon within the first 24 hours.[66,67] The use of functional MRI techniques such as diffusion and perfusion studies for the detection of acute infarction is currently being investigated and is discussed in the article by Tidwell & Jones in the May 1999 issue.

After the first 24 hours, the hyperintensity on T2-weighted and proton density–weighted images becomes more obvious (Fig 9).[64,66,68] During this time, T1-weighted images may show decreased signal.[64,66 68] Gyral swelling and mass effect are more prominent, becoming maximal 2 to 4 days after onset of occlusion.[64 66] Parenchymal enhancement becomes evident within 4 to 7 days and may persist for 3 to 4 weeks.[66] After several weeks, the signal changes seen on earlier scans become smaller and better defined. There is focal atrophy with dilatation of nearby sulci and ventricles. There may be a collection of fluid with the signal characteristics of cerebrospinal fluid.[69] Contrast enhancement does not usually occur.[66]

Hemorrhagic Infarction

The above description applies to nonhemorrhagic or "bland" infarcts. However, many infarcts will have attendant bleeding caused by reperfusion of damaged blood vessels.[66] This results in a hemorrhagic infarct. Petechial hemorrhage into an infarct may result in an isodense lesion on unenhanced CT because of the combined effects of the brain edema, which decreases attenuation, and acute hemorrhage, which increases attenuation. Mass effect caused by the edema usually provides a clue to the presence of a lesion. If hemorrhage is a large component of an acute infarct, unenhanced CT shows a hyperdense hematoma surrounded by hypodense edema. These changes are often confined to a vascular territory, a feature that is helpful in differentiating hemorrhagic infarctions from other causes of hemorrhage.[40] In the subacute phase, the region around the infarct may enhance, increasing the possibility of hemorrhage within a tumor. Mass effect from a hemorrhagic infarct is usually minimal or decreasing at the time of maximal contrast enhancement (2 to 4 weeks), which is useful in differentiating between hemorrhagic infarct and tumor.[51]

The MRI features of hemorrhagic infarction are similar to those of intraparenchymal hemorrhage.[40] Compared with other causes of intraparenchymal hemorrhage, hemorrhagic infarcts tend to have a higher Po_2 because of earlier revascularization and collateral perfusion. The higher Po_2 decreases the amount of deoxyhemoglobin, and therefore minimizes the acute T2 relaxation effect.[51]

Hippocampal Injury After Seizures

Uncontrolled seizures or status epilepticus may result in neuronal degeneration progressing to necrosis. The distribution of lesions varies somewhat among individual patients, but the hippocampus, basal nuclei, and frontal and pyriform lobes of the cerebrum are most severely affected.[70] Lesions are usually bilateral, but may affect one side more severely.[70] These changes are thought to be the consequence of ischemia secondary to accumulation of cytotoxic agents and a mismatch between brain metabolism and blood flow during prolonged seizures.[71]

Persistent or reversible MR lesions have been described in human patients after seizures, and similar abnormalities have

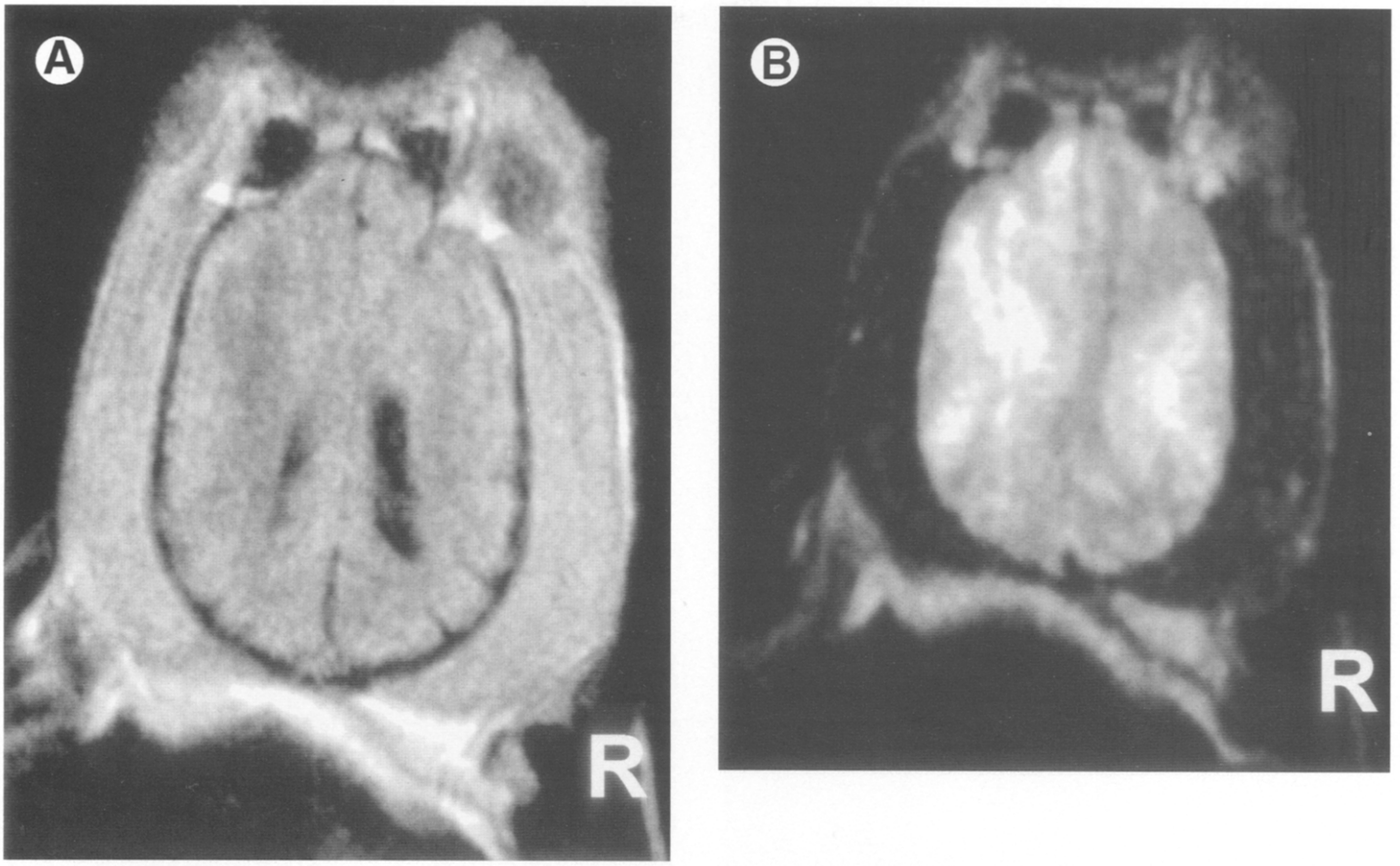

Fig 9. Brain infarct in a dog 6 days after a sudden onset of seizures and right hemiparesis. (A) Dorsal postcontrast T1-weighted MR image shows a subtle decrease in intensity of the left cerebral hemisphere. There is a mass effect evident as compression of the left lateral ventricle and effacement of adjacent sulci. SE, 68/24, 0.064 T. (B) Dorsal T2-weighted image shows a wedge-shaped, hyperintense lesion in the vascular territory of the left middle cerebral and left rostral cerebral artery. There is also a smaller wedge-shaped region of hyperintensity in the vascular territory of the right middle cerebral artery. SE, 1500/105, 0.064 T.

been described in dogs.[72-74] The most consistent finding is unilateral or bilateral lesions of the hippocampus, pyriform lobe, and frontal lobe. The lesions are hypointense on T1-weighted images and hyperintense on proton density–weighted and T2-weighted images. There is minimal mass effect and no or moderate contrast enhancement[74] (Fig 10). These lesions may persist or disappear on subsequent scans.

Head Trauma

Head trauma results from a variety of causes, including motor vehicle accidents, bites, kicks, and gunshot wounds. Previously, imaging of head trauma was limited to skull radiography for the detection of fractures. Plain radiography, however, cannot identify many traumatic brain lesions, such as hemorrhage, and therefore provides only limited diagnostic information. The development of CT provided a sensitive means for detecting and localizing intracranial hemorrhage, permitting expeditious surgical treatment, and improving outcome.[75] MRI has been shown to be similar in sensitivity for detection of hemorrhagic lesions, but is much more sensitive than CT for detecting nonhemorrhagic lesions, such as shearing injuries of white matter.[75]

Neuroimaging should be considered early in the management of animals with head injury and marked impairment of consciousness or neurological deficits that progressively worsen despite initial medical therapy. The most critical issue is to detect potential hematomas that may be treatable with surgery.[76] In general, CT is the diagnostic study of choice for initial evaluation, because it can be completed quickly and is sensitive to acute hemorrhage.[76] CT also provides fine anatomic detail of bone when viewed at a wide window width allowing accurate characterization of any skull fractures[77] (Fig 11).

Although MRI is slightly more sensitive than CT for detection of hematomas, those that are not seen on CT are usually small and typically managed conservatively.[75] A disadvantage of MRI is the longer examination time and the difficulty in monitoring unstable patients in the MRI environment. Therefore, if CT is available, MR examination is usually delayed until the patient is stabilized. In patients with severe head trauma, MRI should be considered in the first 2 weeks after injury, because most parenchymal lesions are more easily detectable during this period.[75]

Epidural Hematoma

Epidural hematomas accumulate in the potential space between the inner surface of the skull and the dura mater. They are usually found in the temporoparieteal region, and have been caused by laceration or tearing of the middle meningeal artery by skull fracture. The arterial force of the bleeding dissects the dura away from the bone, often resulting in a rapidly expanding mass. Clinical signs may consist of rapidly progressing focal neurological deficits and deterioration in

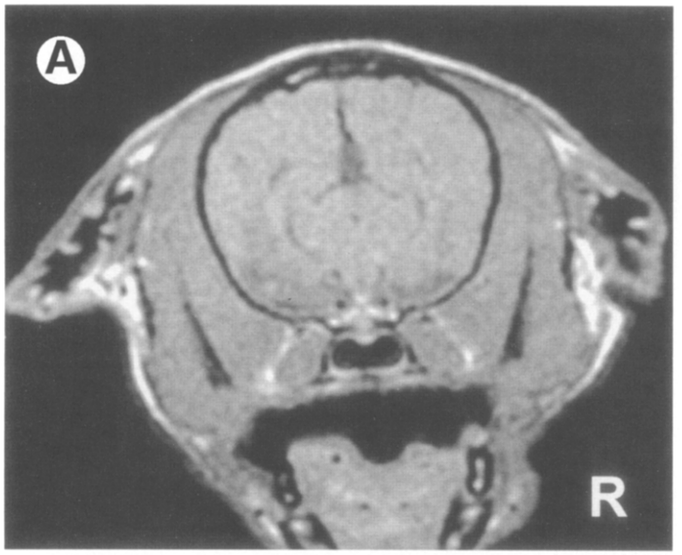

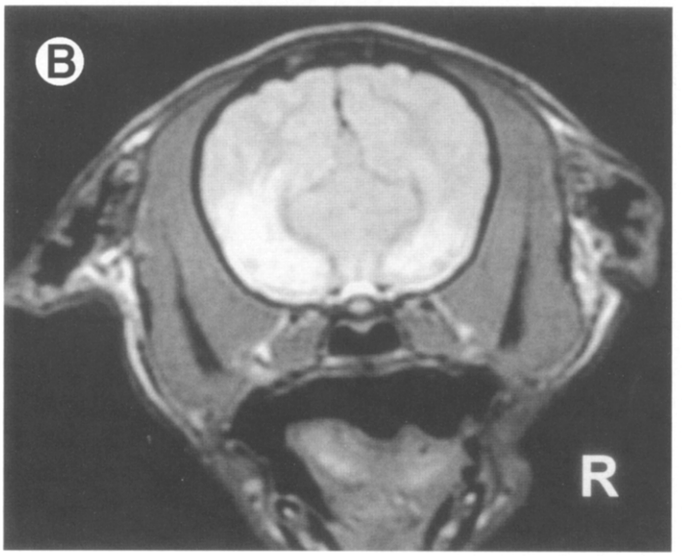

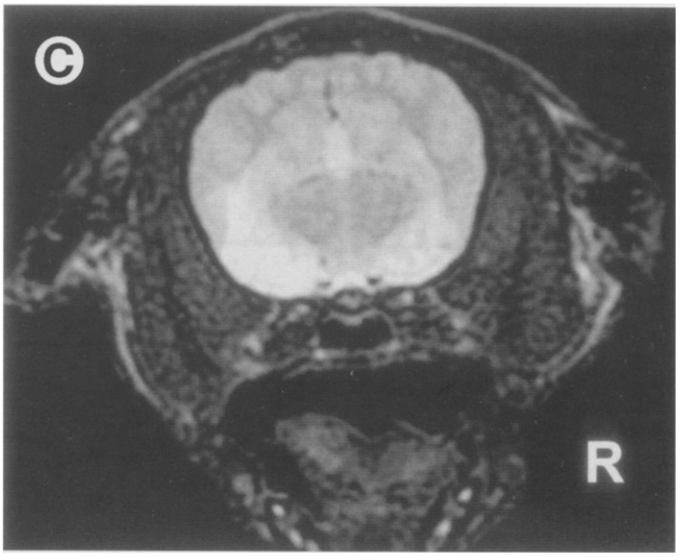

Fig 10. Bilateral forebrain lesions 4 days after an episode of status epilepticus. (A) Transverse T1-weighted MR image shows decreased intensity in the pyriform lobes bilaterally. SE, 600/20, 0.5 T. (B) Transverse proton density–weighted MR image at the same level shows increased intensity of the pyriform lobes. SE, 3000/40, 0.5 T. (C) Transverse T2-weighted image at the same level shows that the lesions are hyperintense. SE 3000/100, 0.5 T. Although no further seizures were noticed, the dog was euthanized 2 weeks later because of persistent abnormal behavior. At necropsy, there was necrosis of the pyriform lobes. No other lesions were found to account for the seizure.

consciousness. However, patients with associated parenchymal brain injury may have severely impaired consciousness at the time of trauma.[75] On CT, an acute epidural hematoma is typically a well-defined, biconvex lesion between the inner table of the skull and the underlying depressed dura and brain.[78] The attenuation of the hematoma is initially greater than brain parenchyma and increases further during the first few hours with coagulation and clot retraction. With time, the attenuation decreases with clot retraction, erythrocyte lysis, and hemoglobin degradation. The hematoma becomes smaller and fades to isodense and then hypodense within 1 or 2 weeks. The inner surface of an epidural hematoma is dura mater, which normally enhances with intravenous contrast material, but this enhancing margin becomes even more prominent as a neovascular membrane develops over time.[78] On MRI, the intensity varies depending on the age of the hematoma, as described in the section on intracranial hemorrhage and summarized in Table 1.

Occasionally, an epidural hematoma may not have the classic lenticular shape or associated skull fracture, making it difficult to differentiate it from a subdural hematoma. MRI can be helpful in this regard, because the medially displaced dura mater is usually directly visualized as a thin line of low signal separating the hematoma from the underlying compressed brain parenchyma.[75] MRI is also superior in the detection of subacute and chronic hematomas, which may be isodense on CT.[77 78]

Subdural Hematoma

Subdural hematomas accumulate within the potential space between the pia-arachnoid and dura mater. They are usually caused by tearing of veins that traverse the subdural space. Subdural hematomas appear to be less common in dogs and cats with head injury, compared with human patients. Clinical signs may consist of progressive asymmetrical neurological deficits and decreased levels of consciousness. An acute subdural hematoma appears on CT as a hyperdense, crescent-shaped collection conforming to the inner surface of the skull.[78] Mass effect is evident and may be compounded by contusion and edema of the underlying brain parenchyma. Acute hyperdense hematomas may not be visible on a narrow window width (soft tissue window), appearing only as an apparent thickening of the skull, since the bone and hematoma may have the same pixel brightness.[75 78] Mass effect is usually present, however, providing a clue in their detection. Widening the window width may be necessary to distinguish an acute subdural hematoma from the dense skull.[78]

As with other intracranial hematomas, the density of a subdural hematoma decreases over time, becoming isodense to

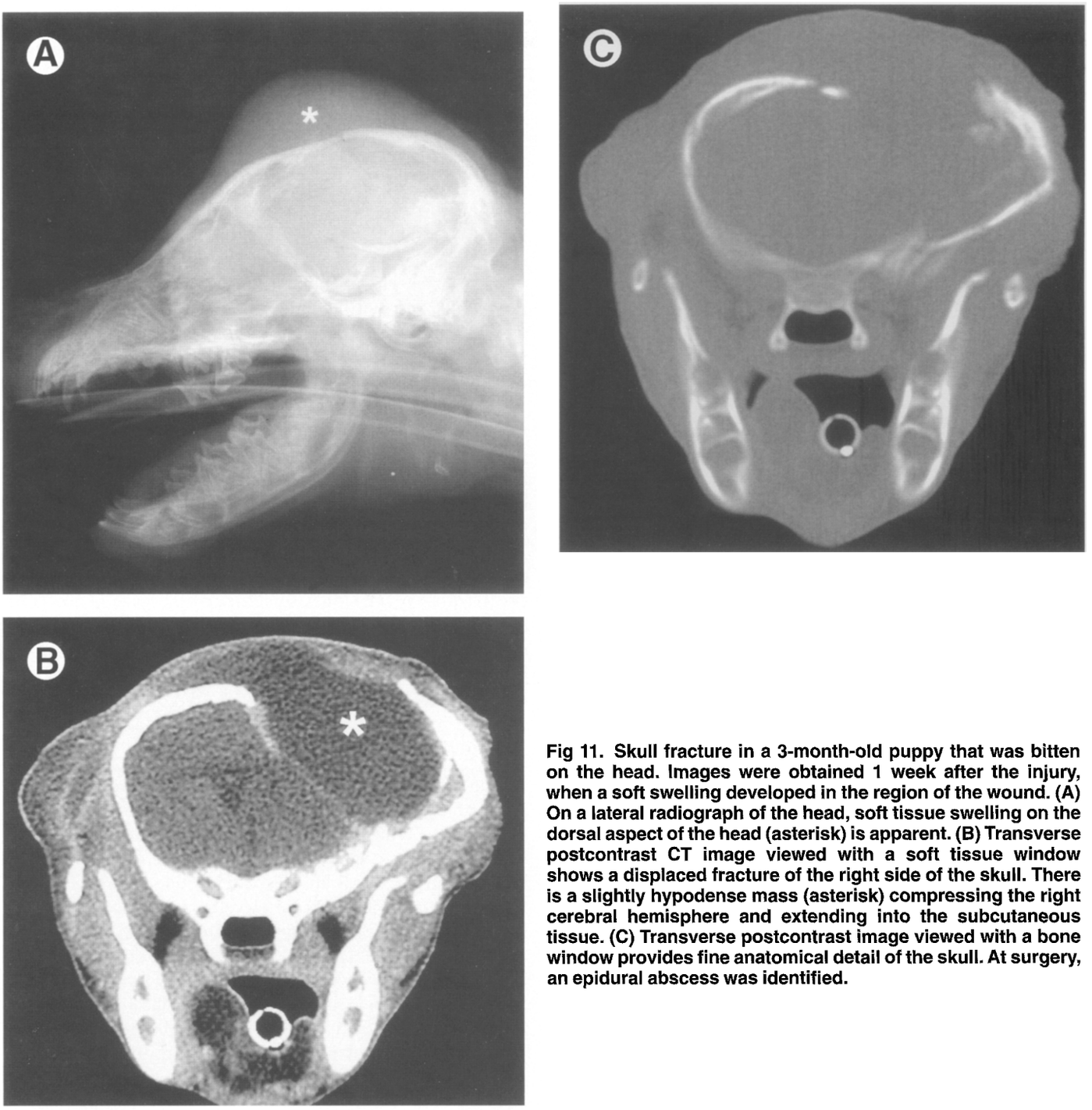

Fig 11. Skull fracture in a 3-month-old puppy that was bitten on the head. Images were obtained 1 week after the injury, when a soft swelling developed in the region of the wound. (A) On a lateral radiograph of the head, soft tissue swelling on the dorsal aspect of the head (asterisk) is apparent. (B) Transverse postcontrast CT image viewed with a soft tissue window shows a displaced fracture of the right side of the skull. There is a slightly hypodense mass (asterisk) compressing the right cerebral hemisphere and extending into the subcutaneous tissue. (C) Transverse postcontrast image viewed with a bone window provides fine anatomical detail of the skull. At surgery, an epidural abscess was identified.

gray matter by 1 to 2 weeks. Accordingly, subacute subdural hematomas may be difficult to detect on CT but are readily detectable on MRI.[75] A chronic subdural hematoma (2 to 3 weeks old or older) is hypodense compared with normal brain on CT and is surrounded by a well-defined capsule (Fig 12). This results in a more focal collection of blood with a straighter medial edge compared with crescent-shaped acute subdural hematomas.[78] The capsule of a chronic subdural hematoma enhances with intravenous contrast material and may calcify.[78]

Subarachnoid Hemorrhage

Subarachnoid hemorrhage is bleeding into the CSF-filled subarachnoid space. Posttraumatic subarachnoid hemorrhage is relatively common and often associated with cortical contusions. Acute subarachnoid hemorrhage is evident on CT as increased attenuation of the sulci, fissures, or basal cisterns, with the degree of increased attenuation being related to the amount of blood in the subarachnoid space.[78] With time the attenuation decreases and subarachnoid hemorrhage may not be detectable after the first week, unless rebleeding has occurred.[51] Acute subarachnoid hemorrhage is usually not detectable on MRI, probably because the Po_2 of the subarachnoid CSF is too high for the conversion of oxyhemoglobin to deoxyhemoglobin and methemoglobin.[51] However, MRI is excellent at detecting subarachnoid hemorrhage in the subacute or chronic stage.[51]

Contusion

Brain contusions are common after head trauma and consist of heterogeneous regions of hemorrhage, edema, and necrosis,

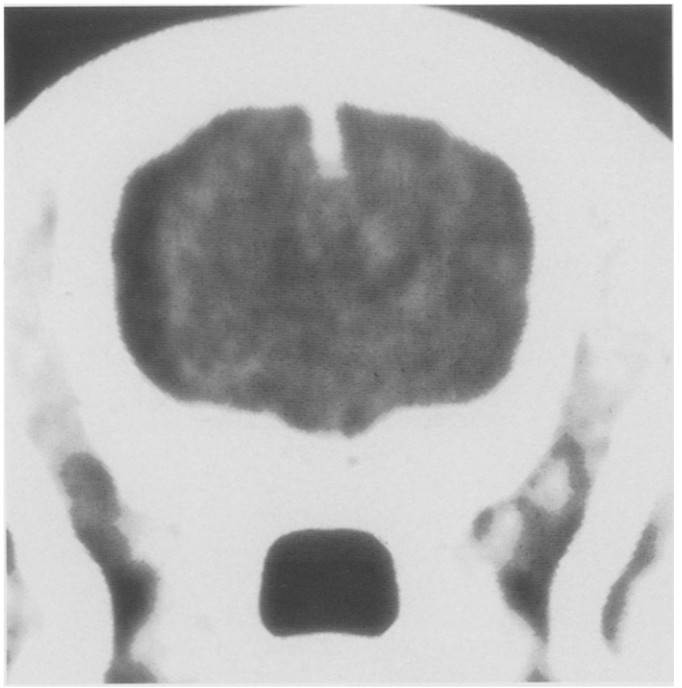

Fig 12. Transverse postcontrast CT image of a dog with a chronic subdural hematoma secondary to head trauma occurring 14 days earlier. A crescent-shaped collection of hypodense fluid is present between the skull and underlying left cerebral hemisphere. There are scattered regions of enhancement of the cerebral cortex subjacent to the hematoma and a shift of the midline to the right. Surgery confirmed a subdural hematoma.

often located in the superficial gray matter. In human patients contusions tend to be multiple and bilateral and are much less likely to be associated with severe initial impairment of consciousness compared with diffuse axonal injury.[75] Initial CT findings are often limited to faint, ill-defined hypodense areas mixed with tiny regions of hyperdense hemorrhage.[75] Contusions in which edema and necrosis predominate may not be visible initially on CT but often become apparent several days later as regions of decreased attenuation and mass effect caused by edema.[78] MRI, because of its greater sensitivity in detecting edema, is better at detecting early contusions, which appear hypointense on T1-weighted images and hyperintense on T2-weighted images.[75]

Diffuse Axonal Injury

Head trauma that involves rapid angular acceleration may result in diffuse axonal injury. These shearing injuries result from differences in elastic and inertial properties between different but adjacent brain tissues.[78,79] In human patients, these injuries are characterized pathologically by disruption of axons, especially at the junction of gray and white matter of the cerebrum, and at the corpus callosum, basal nuclei, and cranial aspect of the brainstem. There is subsequent axonal swelling and infiltration with macrophages. These patients present with severe impairment of consciousness starting from the moment of injury.[76,77,80]

MRI is much more sensitive than CT in detecting diffuse axonal injury in human patients, although even MRI findings usually underestimate the true extent of these injuries.[75] CT is often normal, but may show scattered hemorrhages. The MRI appearance reflects the prolonged T1 and T2 values of increased tissue fluid (edema). There are multiple, small elliptical lesions in the white matter. These lesions are hypointense on T1-weighted images and hyperintense on T2-weighted images.[75,78]

Infectious and Inflammatory Diseases

Inflammatory diseases are important diagnostic considerations for patients with brain disease. Infectious agents, such as viruses, protozoa, and fungi, cause many inflammatory diseases, but for others the etiology is unknown. Despite the numerous causes of inflammatory brain disease, the affected tissue can respond only in a limited number of ways. Thus, many of these diseases appear similar on imaging studies and differentiating the potential etiologies based on imaging features alone may be impossible. Furthermore, it may be difficult to discriminate between inflammatory diseases and other categories of disease, such as neoplasia and vascular disorders. Accordingly, results of imaging studies must be interpreted in context with clinical features and results of other laboratory tests, especially analysis of CSF.[81]

All inflammatory brain diseases share a common pathological feature—an influx of leukocytes into the brain (cerebritis or encephalitis) or meninges (meningitis). Because of the close anatomical association of these structures, more than one area of the nervous system can be involved in the inflammatory process. For example, inflammation of the meninges and brain is called meningoencephalitis.[82]

Meningitis

The most common cause of meningitis in dogs is steroid-responsive meningitis-arteritis, a nonseptic suppurative meningitis of unknown etiology that responds to immunosuppressive dosages of corticosteroids.[83] Infectious causes of meningitis are less common in small animals and include bacteria, viruses, fungi, and protozoa.[84] Pathologically, acute leptomeningitis results in congestion and hyperemia of the pia-arachnoid and distension of the subarachnoid space by an exudate containing leukocytes. Clinically, affected patients show fever, spinal pain, cervical rigidity, and stiff gait. Several complications can occur in the ensuing days to weeks. There may be extension of the infection to the neural parenchyma, resulting in focal or diffuse encephalitis, myelitis, or abscess. Inflammatory exudate may obstruct CSF pathways, producing hydrocephalus. Endogenous host inflammatory mediators can result in disruption of the blood-brain barrier, cerebral edema, and increased intracranial pressure.[85] Definitive diagnosis of meningitis is based on analysis of CSF. Neuroimaging is useful in detecting some of the complications associated with meningitis and when the differential diagnosis includes other diseases.

Neuroimaging features of experimental bacterial meningitis in dogs is comparable with naturally occurring bacterial meningitis in human patients.[86,87] In human patients with uncomplicated early bacterial or viral meningitis, unenhanced CT and MRI are often unremarkable or show mild dilatation of the ventricles or subarachnoid space (Fig 13).[88] With more severe involvement, there may be diffuse or patchy brain edema.[88] Postcontrast CT or MRI may show abnormal enhancement of the leptomeninges.[89] In experimental studies in dogs, T1-weighted MR images with gadolinium showed abnormal

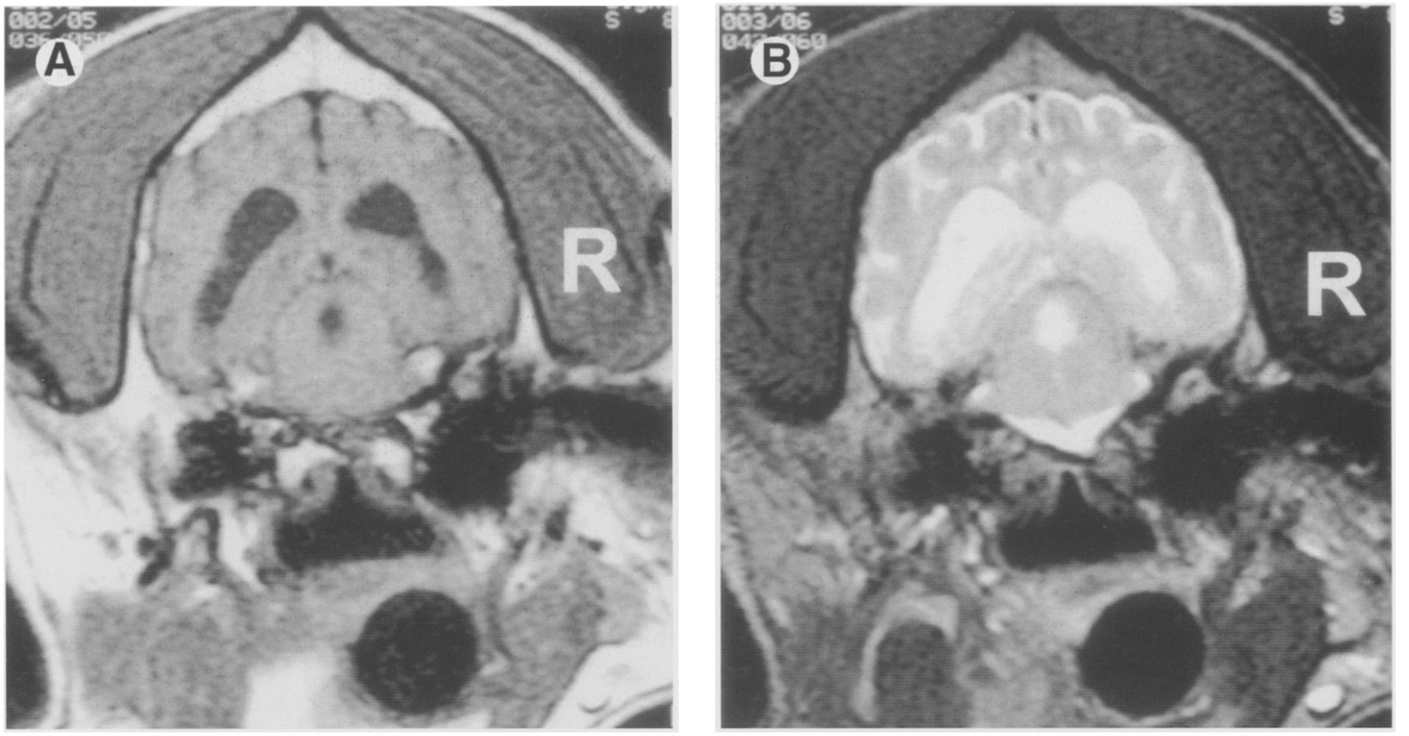

Fig 13. Bacterial meningitis in a dog. (A) The transverse noncontrast T1-weighted MR image is normal, except for enlargement of the lateral ventricles and mesencephalic aqueduct. SE, 500/19, 1.5 T. (B) Transverse T2-weighted image shows hyperintensity of the leptomeninges/subarachnoid space. SE, 2500/80, 1.5 T.

leptomeningeal enhancement better than CT.[87] MRI also identifies complications such as encephalitis more effectively than CT.[87]

Encephalitis

Encephalitis generally refers to nonpurulent inflammation of the brain and is distinguished pathologically from suppurative inflammation of the brain (cerebritis) associated with bacterial infection.[88] Viral encephalitides of small animals include canine distemper and feline infectious peritonitis. Other causes of encephalitis include Rocky Mountain Fever, canine ehrlichiosis, toxoplasmosis, and neosporosis. Finally, there are encephalitides of unknown etiology, such as pug dog encephalitis and granulomatous meningoencephalitis.

Distemper encephalitis. The two most common clinical forms of distemper encephalitis are acute encephalitis in young dogs and chronic encephalitis in mature dogs. Immature dogs with distemper encephalitis typically suffer a rapid onset of systemic illness characterized by conjunctivitis, nasal discharge, cough, vomiting, and diarrhea. Neurological dysfunction can occur during or after the systemic illness and includes seizures, abnormal behavior, blindness, and paresis. Mature dogs are more likely to develop chronic, multifocal encephalitis with a predilection for the white matter of the brainstem. Many of these dogs have an adequate vaccination history, and signs of systemic illness are often absent or transient.[90-92] These patients often have slowly progressive gait deficits or vestibular dysfunction.[90,91]

CT of dogs with chronic distemper encephalitis may be normal or show focal or multifocal hypoattenuating lesions with a predilection for the white matter.[93] These lesions may have uniform or ring-like enhancement[93] (Fig 14). Some

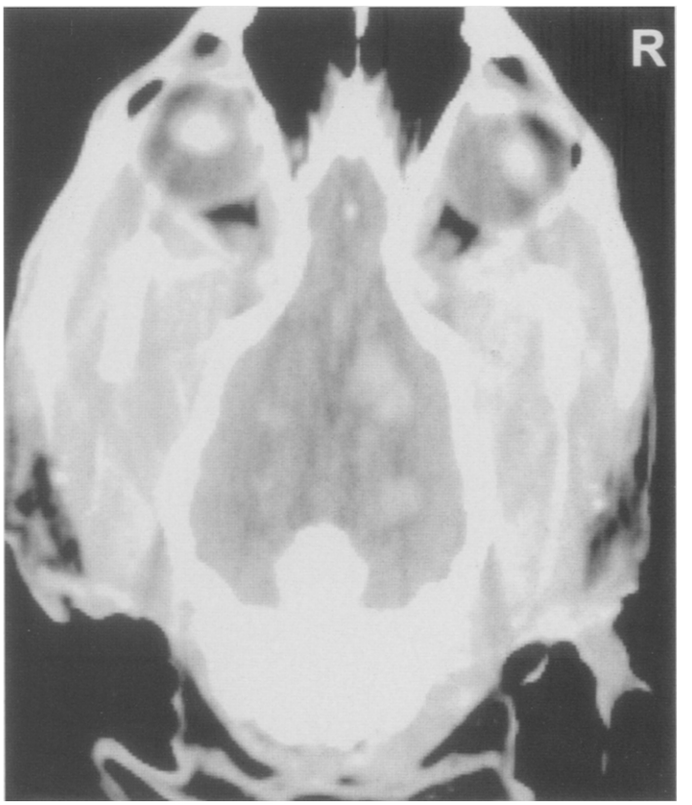

Fig 14. Distemper encephalitis in a mature dog. On the dorsal postcontrast CT image, there are multiple, variable-sized regions of abnormal enhancement. Multifocal meningoencephalitis caused by canine distemper virus was identified on postmortem examination.

lesions may be associated with hypoattenuating edema and mass effect.[93] Lesions are typically hypointense or poorly defined on T1-weighted MRI, hyperintense on T2-weighted images, and enhance with contrast agent.[94]

Feline infectious peritonitis. Feline infectious peritonitis (FIP) is a systemic disease of cats caused by an immune response to a corona virus. Neurological signs are generally associated with the parenchymatous (dry) form of FIP. Neurological deficits referable to brainstem involvement predominate and include ataxia, paresis, and vestibular dysfunction.[95-97]

Imaging features of FIP reflect the pathological changes, which consist of pyogranulomatous inflammation of the leptomeninges, choroid plexus, ependyma, and brain parenchyma. Hydrocephalus is common and is probably secondary to obstruction by ependymitis.[95-98] The brainstem and fourth ventricle are consistently involved, but other regions of the central nervous system can be affected.[95,96] The inflammatory process primarily affects the inner and outer surfaces of the brain with only secondary extension into the parenchyma. Recognition of this surface-related pattern can be helpful in differentiating FIP from other brain diseases in the cat.[98] CT may be normal or show hydrocephalus.[95] MRI may show ependymitis, choroiditis, and meningitis. This is evident as hyperintensity of the ventricular lining, choroid plexus, and meninges, respectively, on T2-weighted MRI and abnormal enhancement with gadolinium-based contrast agent[97,99] (Fig 15).

Fungal infections. Many fungal agents can sporadically infect the nervous system, causing meningitis or granulomas. *Cryptococcus neoformans* is the most common fungal infection to involve the nervous system of dogs and cats. In cats, this organism generally induces a mild, nonsuppurative meningitis or encephalitis, whereas affected dogs typically develop a granulomatous reaction in the brain and meninges.[98] Neurological deficits can be acute or chronic and include seizures, lethargy, ataxia, and vestibular dysfunction.[100,101] On CT, mass lesions (cryptococcomas) appear as single or multiple isodense or hypodense masses with ring or solid enhancement and surrounding edema.[81,89,93,102] Leptomeningeal enhancement may also be apparent if the meninges are involved.[81,102] Hydrocephalus may occur secondary to meningitis or obstruction of CSF pathways by the mass.[81,89] In human patients, MRI is more sensitive than CT and may show clustered foci of signal abnormalities that are isointense to CSF on all sequences. These lesions represent small granulomas or dilated Virchow-Robin spaces filled with fungal organisms and mucoid. These are often bilaterally symmetrical, and are located in the basal nuclei and midbrain. These lesions do not enhance with gadolinium and are not associated with mass effect or edema.[89] Similar changes have been reported on MRI of canine cryptococcosis.[103] Cryptococcomas appear as masses that are hypointense on T1-weighted images, hyperintense on T2-weighted images, and enhance with gadolinium.[89,103]

Other fungal organisms sporadically infect the central nervous system, including *Blastomyces dermatidis, Histoplasmosis capsulatum, Aspergillus* spp, *Coccidiodes immitis,* and phaeohyphomycosis (Fig 16).[104-111]

Necrotizing encephalitis (pug dog encephalitis). A necrotizing form of encephalitis has been recognized in pug dogs, Maltese terriers, and Yorkshire terriers between 6 months and 10 years of age.[112-116] Signs include progressive seizures, abnormal behavior, blindness, ataxia, and walking in circles. Pathological changes consist of multifocal necrosis and nonsuppurative inflammation, with a striking predilection for the white matter of the cerebrum. Lesions are often bilateral but asymmetrical.[112-114,116] Enlargement of the lateral ventricles secondary to shrinkage and cavitation of the cerebral hemispheres (hydrocephalus ex vacuo) is common[112,114,116] (Fig 2). In Yorkshire terriers, the brainstem may be preferentially involved.[113] The etiology is unknown.

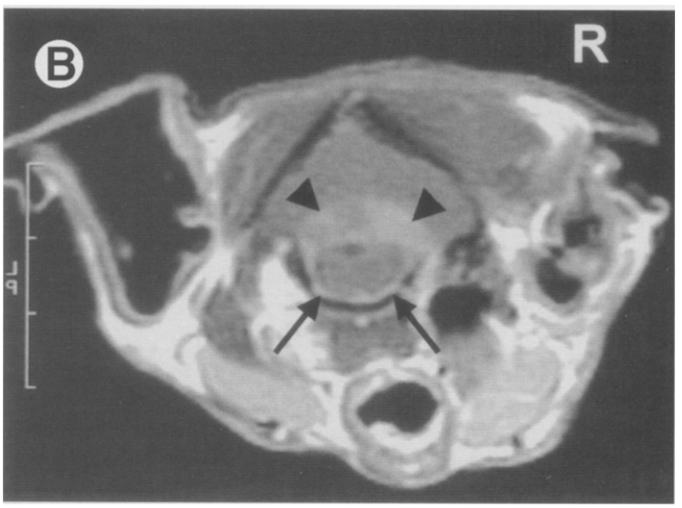

Fig 15. Meningoencephalitis associated with feline infectious peritonitis. (A) Dorsal postcontrast T1-weighted MR image shows enhancement of the choroid plexus (arrowheads) reflecting choroiditis evident at necropsy. SE, 316/10, 1.5 T. (B) Transverse image at the level of the brainstem shows enhancement of the meninges caused by meningitis (arrows) and enhancement of the choroid plexus of the fourth ventricle (arrowheads). SE, 416/10, 1.5 T. (Courtesy of Kim Knowles, DVM, MS; and Amy Tidwell, DVM, Tufts University)

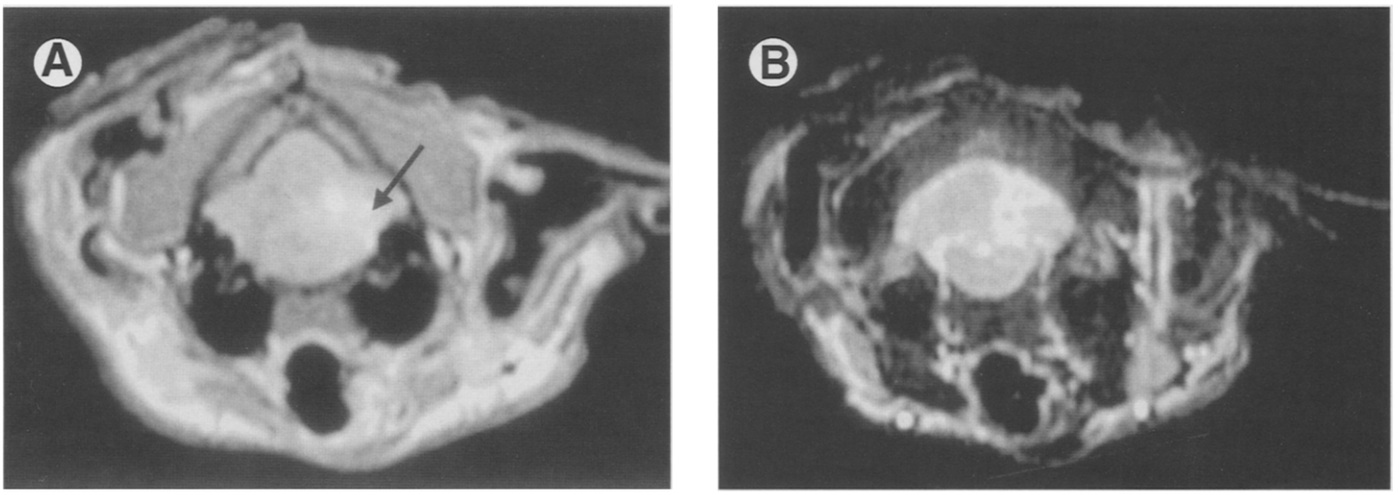

Fig 16. Fungal granuloma caused by phaeohyphomycosis in a cat. (A) Transverse postcontrast T1-weighted MR image shows focal, heterogeneous enhancement in the right cerebellar hemisphere (arrow). SE, 800/25, 0.5 T. (B) On the transverse T2-weighted image, the lesion is hyperintense. SE, 2,000/100, 0.5 T. Necropsy confirmed pyogranulomatous meningoencephalitis caused by *Xylohypha bantianum*.

In acute forms of the disease, CT may show one or more focal hypodense lesions, most commonly affecting the cerebral hemisphere. The lesions may or may not enhance with contrast agent. MRI shows the early edematous changes as increased signal intensity on proton density–weighted and T2-weighted images and decreased signal intensity on T1-weighted images. In acute cases, there is often substantial mass effect and minimal if any abnormal enhancement with contrast medium (Fig 17). Differentials include neoplasia, other inflammatory lesions, and acute infarction.

In more chronic cases, necrosis and cystic changes usually predominate. The centers of the lesions appears similar to CSF; that is, hypodense on CT, very hypointense on T1-weighted images, and very hyperintense on proton density–weighted and T2-weighted images[114-116] (Fig 18). Lesions are usually located in the white matter of the cerebral hemisphere, often in the area lateral to the ventricles.[113] Typically there is no mass effect or even a reverse mass effect (shift of surrounding tissue toward the lesion). Lesions usually do not enhance, but may have a ring pattern of enhancement.[93,114,115] Asymmetric enlargement of the lateral ventricles is common.[93] The primary differential is chronic infarction. However, in necrotizing encephalitis the lesions are not confined to a specific vascular territory as is typical of infarction caused by thromboembolism. The onset of signs (sudden in infarction versus slow onset in chronic necrotizing encephalitis) is also helpful.

Granulomatous meningoencephalomyelitis. Granulomatous meningoencephalomyelitis (GME) is an inflammatory disease of the canine central nervous system characterized pathologically by an accumulation of mononuclear cells in the parenchyma and meninges of the brain and spinal cord.[117] Lesions may be disseminated or focal. In the disseminated form, lesions are distributed throughout the central nervous system, with a predilection for the white matter of the cerebrum, cerebellum, caudal aspect of the brainstem, and cervical spinal segments. The focal form is manifested as a single granulomatous mass, most commonly located in the cerebrum, with smaller disseminated lesions.[118-121] The cause is not known.

Adult dogs of any breed can be affected, although females and toy and terrier breeds are at increased risk.[118-122] Dogs with disseminated GME usually have rapidly progressive signs including neck pain, vestibular dysfunction, paralysis, and seizures. The focal form is manifested as chronic, gradually progressive signs, with seizures being the most common.[118-123] The clinical presentation of focal GME often mimics that of a tumor.

On CT, disseminated GME is seen as multiple foci of ill-defined contrast enhancement involving the parenchyma and meninges. Some lesions may be associated with hypoattenuating edema and mass effect.[124] Other inflammatory diseases are the primary differentials. Focal GME appears on noncontrast CT as an isodense or hyperdense mass, most commonly located within the cerebrum or at the cerebellomedullary junction (Fig 19).[93,125] On MRI, focal GME is usually isointense or slightly hypointense on T1-weighted images and hyperintense on proton density–weighted and T2-weighted images (Fig 20).[126] Enhancement is variable, including no enhancement, ring-pattern enhancement, or moderate homogenous enhancement.[93,124,125] There may be edema in the white matter surrounding the mass.[93,125,126] Asymmetric enlargement of the lateral ventricles has also been reported.[93] The primary differentials are neoplasia and other inflammatory lesions. Biopsy is often necessary for definitive diagnosis.[125]

Bacterial Cerebritis and Abscess

Focal infection of the brain with pyogenic organisms is uncommon in small animals. Bacteria may gain access to the brain through penetrating wounds; secondary to direct extension from infections in the eye, ear, nasal passages, or meninges; or via hematogenous spread from extracranial sources.[127,128] With hematogenous spread, lesions often arise at the gray–white matter junction of the cerebrum.[88] Clinical signs reflect a progressively worsening focal brain lesion.[127,128]

Several reports detail the pathological and CT features of experimental cerebritis/abscess in dogs.[129,130] These imaging features are similar to those reported in human patients with spontaneous brain abscess.[131] Pathologically, serial changes occur over 2 to 3 weeks, starting as cerebritis and culminating in abscess. Focal but poorly localized areas of scattered necrosis, edema, vascular congestion, and perivascular inflam-

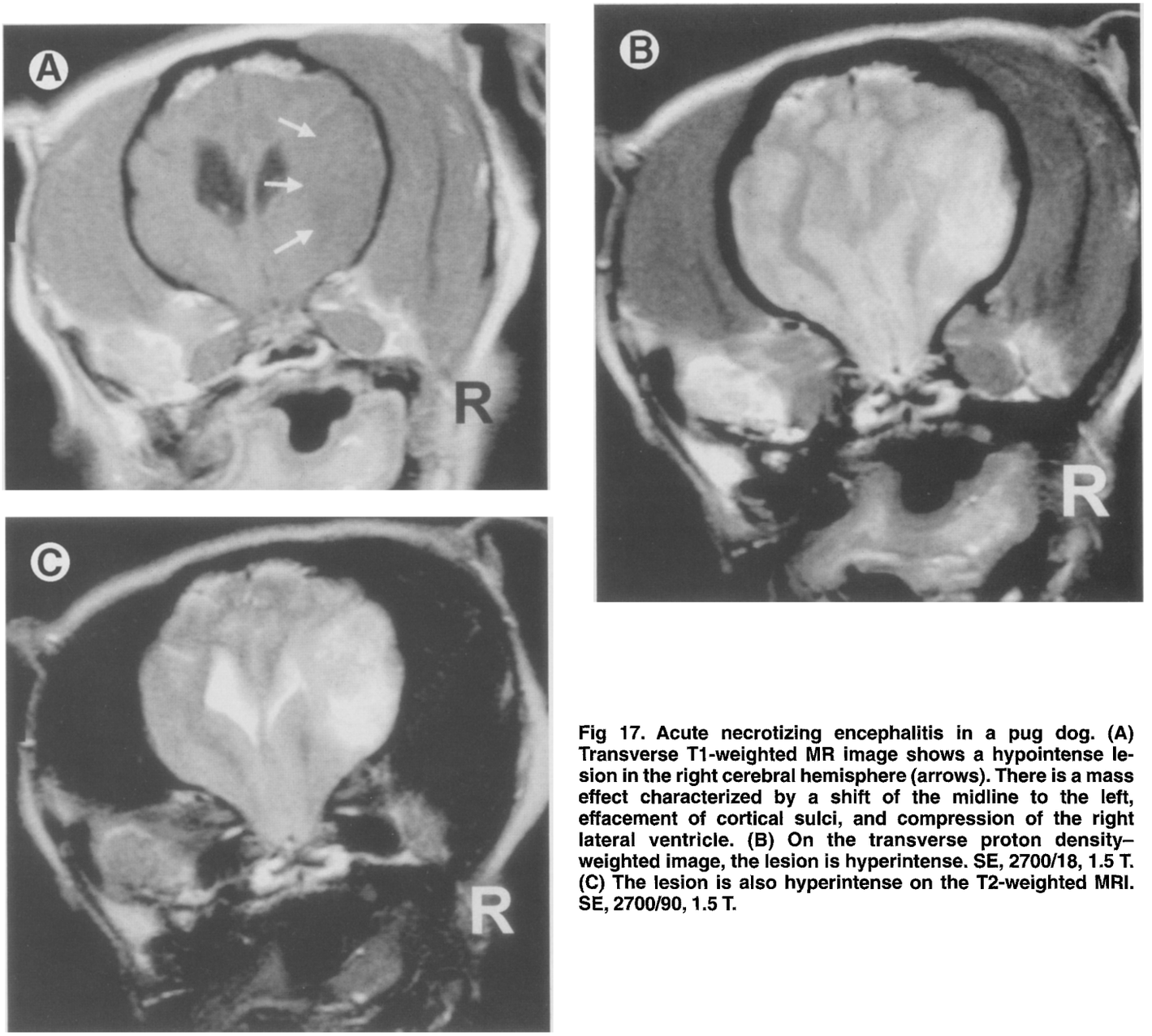

Fig 17. Acute necrotizing encephalitis in a pug dog. (A) Transverse T1-weighted MR image shows a hypointense lesion in the right cerebral hemisphere (arrows). There is a mass effect characterized by a shift of the midline to the left, effacement of cortical sulci, and compression of the right lateral ventricle. (B) On the transverse proton density–weighted image, the lesion is hyperintense. SE, 2700/18, 1.5 T. (C) The lesion is also hyperintense on the T2-weighted MRI. SE, 2700/90, 1.5 T.

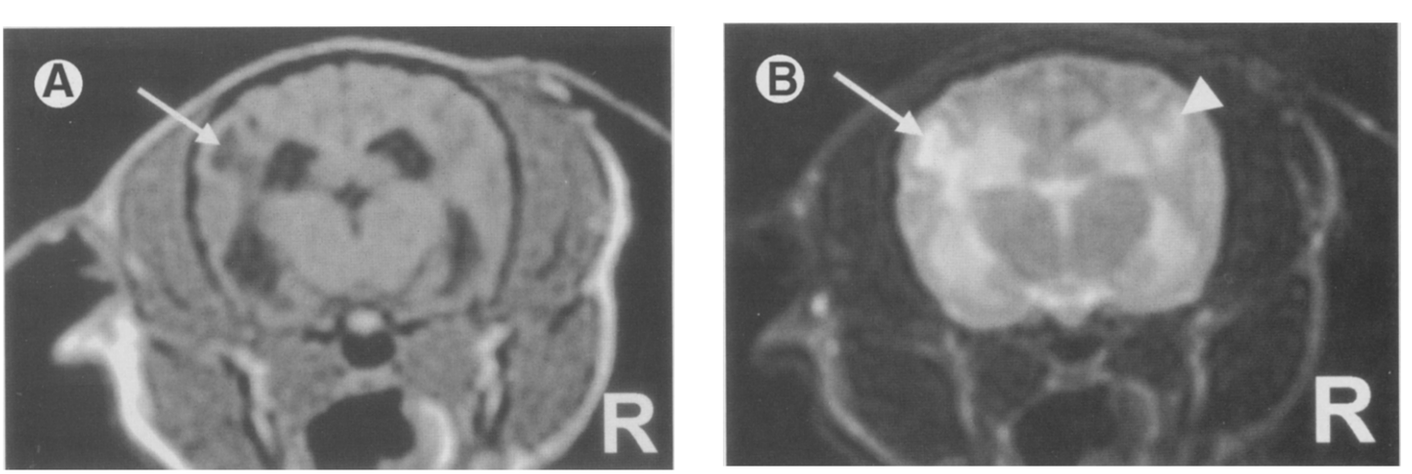

Fig 18. Chronic necrotizing encephalitis in a Yorkshire terrier with a 3-month duration of blindness referable to a forebrain lesion. (A) Transverse postcontrast T1-weighted MR image shows a hypointense lesion (arrow) in the white matter adjacent to the left lateral ventricle. There is no mass effect or abnormal enhancement. SE, 330/12, 0.5 T. (B) Transverse T2-weighted image shows that the lesion (arrow) is well defined, confined to the white matter, and has an intensity similar to CSF. There is a second lesion (arrowhead) in the white matter immediately lateral to the right lateral ventricle. SE, 2600/100, 0.5 T.

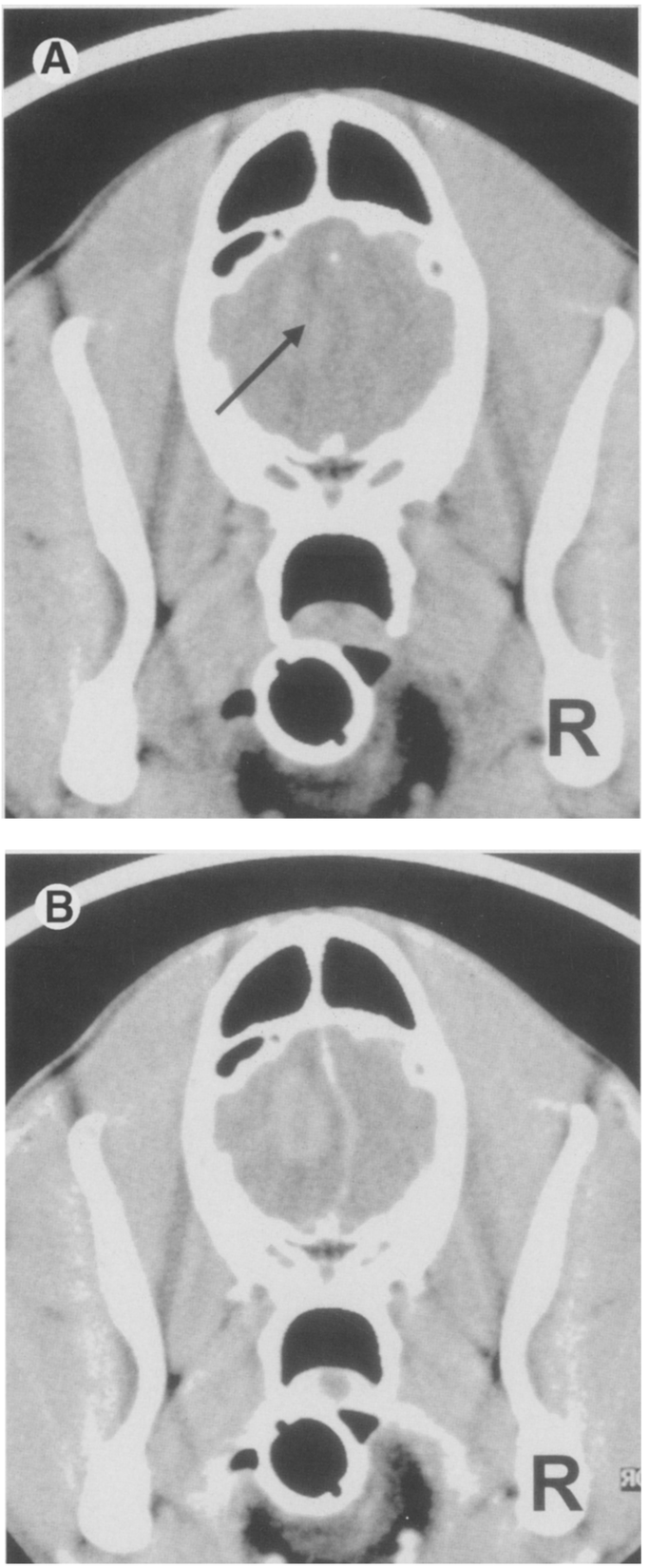

Fig 19. Focal granulomatous meningoencephalitis in a dog with a recent onset of seizures. (A) Transverse noncontrast CT image shows a slightly hyperdense mass (arrow) in the left frontal lobe. The mass is surrounded by a hypodense region, probably representing edema. (B) Transverse postcontrast image shows focal enhancement of the lesion. There is an associated mass effect evident as displacement of the falx to the right. Biopsy confirmed idiopathic granulomatous meningoencephalitis.

matory infiltrates characterize cerebritis. At this stage, unenhanced CT shows only an irregular, poorly circumscribed region of low attenuation.[129-132] Scans obtained immediately after contrast administration show ring-like enhancement. On delayed scans, contrast diffuses into the center of the lesion, starting peripherally, until the center of the lesion may be completely filled with contrast by 30 minutes after administration.[129-131] The inherent sensitivity of proton density–weighted and T2-weighted MRI to alterations in tissue water enables earlier detection of cerebritis compared with CT.[89,132] These images show increased signal intensity indistinguishable from or slightly hypointense to surrounding edema.[89,132] On T1-weighted images, cerebritis is isointense to slightly hypointense to adjacent brain parenchyma, with associated mass effect.[89,132]

Over a period of 1 to 2 weeks, untreated cerebritis may progress to abscess formation when the central zone of necrosis becomes liquefied, better defined, and encircled by a collagen capsule, which is formed by fibroblast migration from the surrounding vessels. Because of relatively poor vascularization of white matter, the medial aspect of the capsule may be somewhat thinner. This predisposes to expansion of the abscess into white matter, the formation of daughter abscesses medially, or rupture into the lateral ventricles.[129,130,132] The capsule is visible on unenhanced CT as an isodense rim that is visible because it is bordered medially by a hypodense liquid center and surrounded by hypodense edema (Fig 21).[131] The edema may be greater in volume than the abscess itself, causing much of the mass effect.[131] On contrast-enhanced CT, the rim is usually smooth and brightly enhancing. There is no diffusion of contrast into the necrotic center on delayed scans as there is with cerebritis.[129-131] On T1-weighted MRI there is mild peripheral hypointensity representing edema and a more markedly hypointense liquid center. The capsule is a discrete rim that is isointense to slightly hyperintense. On T2-weighted images the abscess center is isointense to mildly hyperintense to gray matter. The capsule is seen as a dramatic hypointense rim, possibly caused by paramagnetic free radicals within phagocytic macrophages.[89] The ring pattern of enhancement parallels the enhancement seen on contrast-enhanced CT.

The differential diagnosis for a ring-enhancing lesion includes primary brain tumor, metastasis, infarction, granuloma, and resolving hematoma.[42,89] Helpful clues that may identify abscesses include the time course, location, temporal pattern of enhancement, and predisposition for the abscess rim to be thinner medially.[89]

Parasitic Infections

Cuterebra. Dogs and more commonly cats can suffer brain disease caused by aberrant migration of *Cuterebra* larvae.[133-135] Fly larvae attach to the host and burrow into the subcutaneous tissue. The developing larva (1 to 10 mm long) may migrate under the skin and enter the brain, most likely through the nasal passages and cribiform plate.[134,135] Pathological changes in the brain consist of multifocal meningoencephalitis with malacia and hemorrhage.[133-135]

Affected animals typically have access to outdoors and develop signs from June to October, coinciding with the larval migration portion of the *Cuterebra* life cycle. A recent history of upper respiratory disease is common, likely reflecting migration of the larvae through nasal passages.[135] There is an acute

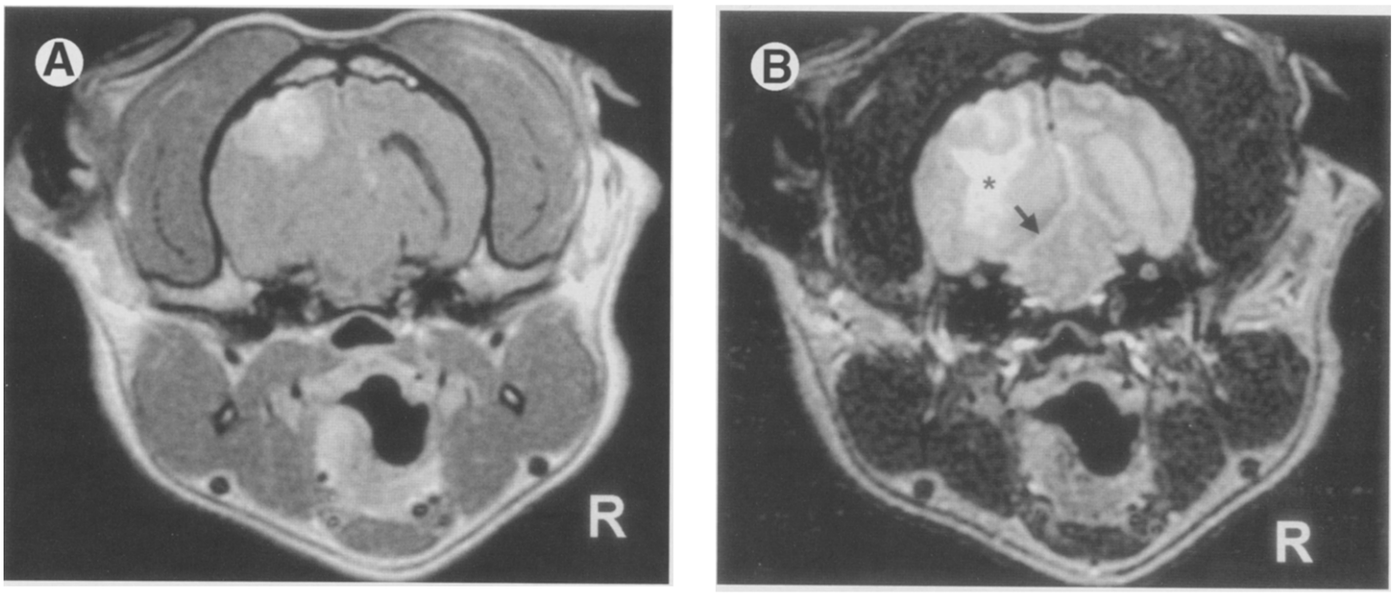

Fig 20. Focal granulomatous meningoencephalitis in a dog. (A) Transverse postcontrast T1-weighted MR image shows an enhancing mass in the dorsal aspect of the left cerebral hemisphere. There is a mass effect, including compression of the left lateral ventricle. SE, 700/20, 0.5 T. (B) On the transverse T2-weighted image, the lesion is isointense to hyperintense. There is hyperintensity of the adjacent white matter (asterisk), due to edema. Note the caudal transtentorial herniation with compression of the left side of the midbrain (arrow). SE, 2,000/80, 0.5 T. Biopsy confirmed idiopathic granulomatous meningoencephalitis. (Reprinted with permission.[82])

onset of neurological dysfunction, most commonly referable to a focal forebrain lesion. Seizures, abnormal mentation, circling, hemiparesis, and unilateral blindness are common.[134,135] Clinical and pathological features in cats are similar to what has been previously reported as feline ischemic encephalopathy.[135]

A mottled appearance to the brain has been reported on CT of an affected cat.[135] Based on my observations, CT may show focal or multifocal regions of decreased attenuation with minimal mass effect. The may be one or more tract-like regions of contrast enhancement (Fig 22). Lesions may be hypointense on T1-weighted MRI and hyperintense on T2-weighted MRI. Edema is fairly minimal, and there may be small regions of hemorrhage. Contrast enhancement is similar to that described for CT.

Coenurosis. The intermediate stage (*Coenurus*) of tapeworms (*Taenia*) can produce fluid-filled cysts in the brains of cats. Lesions are usually located within the cerebrum. As the cyst expands, filling it with fluid, it compresses adjacent neural tissue and causes circling, abnormal behavior, and visual deficits.[136,137] On CT there is a well-defined intraparenchymal mass filled with fluid that is isodense to cerebrospinal fluid. There is little, if any, edema. The cyst wall is thin and smooth

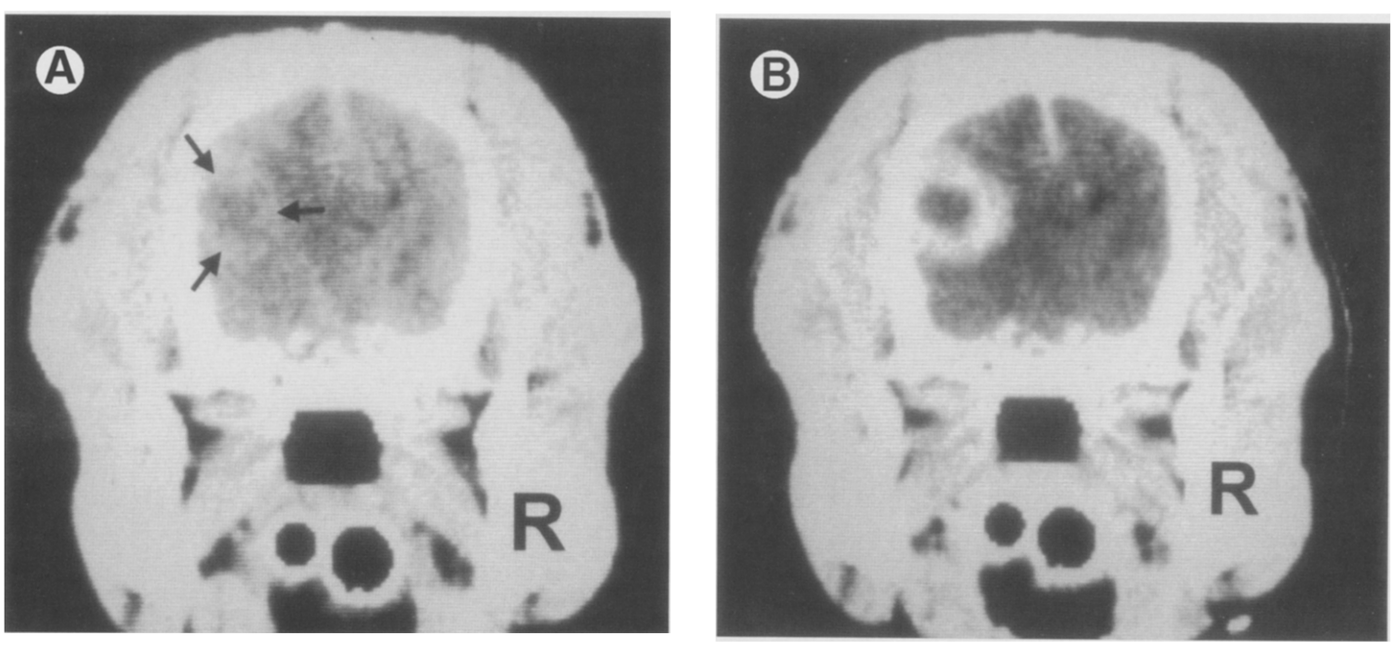

Fig 21. Brain abscess in a dog. (A) Transverse noncontrast CT image shows a mass in the left cerebral hemisphere. The center of the lesion is slightly hypodense and surrounded by a hyperdense rim with uniform thickness. (B) Transverse postcontrast image shows a ring pattern of enhancement. (Courtesy of Rodney Bagley, DVM, Washington State University.)

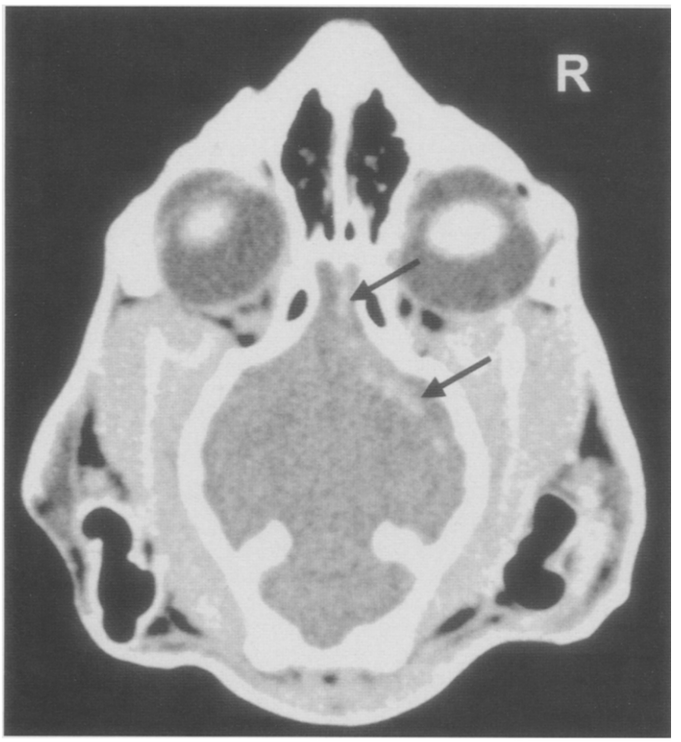

Fig 22. Dorsal postcontrast CT image of a cat suspected of having intracranial migration of a *Cuterebra* larva. An enhancing tract (arrows) extends from the cribiform plate through the right cerebral hemisphere. This cat, which lived outside, presented in October, 5 days after suffering a sudden onset of sneezing followed by seizures, left hemiparesis, depression, and circling to the right. Clinical signs gradually resolved over the next 2 weeks, so the diagnosis was not confirmed by necropsy, but the clinical features are consistent with intracranial migration of a *Cuterebra* larva.

and does not enhance.[136] The intraparenchymal location is helpful in differentiating these lesions from arachnoid cysts, which are associated with the subarachnoid space.[25,26]

Summary

CT and MRI are helpful in identifying and characterizing many nonneoplastic brain disorders in dogs and cats. The imaging features of some of these disorders are unique, permitting definitive diagnosis based on imaging results and clinical features. However, the imaging findings for other brain disorders are nonspecific. In these instances, CT and MRI often allow detection and localization of abnormalities, but definitive diagnosis may require other laboratory tests or surgical biopsy. As the use of CT and MRI becomes more widespread in veterinary medicine, further research in the imaging findings associated with various nonneoplastic disorders will improve our ability to diagnose and manage these conditions.

References

1. Gilman S: Imaging the brain (first of two parts). N Engl J Med 338.812-820, 1998
2. Harrington ML, Bagley RS, Moore MP: Hydrocephalus. Vet Clin North Am 26:843-856, 1996
3. Becker SV, Selby LA: Canine hydrocephalus. Comp Contin Ed Pract Vet 2:647-652, 1980
4. Naidich TP, Schott LH, Baron RL: Computed tomography in evaluation of hydrocephalus Radiol Clin North Am 20:143-165, 1982
5. Kay ND, Holliday TA, Hornoff WJ, et al. Diagnosis and management of an atypical case of hydrocephalus, using computed tomography, ventriculoperitoneal shunting, and nuclear scintigraphy. J Am Vet Med Assoc 188:423-426, 1986
6. Hudson JA, Simpson ST, Buxton DF, et al: Ultrasonographic diagnosis of canine hydrocephalus. Vet Radiol 31:50-58, 1990
7. Spaulding KA, Sharp NJH: Ultrasonographic imaging of the lateral cerebral ventricles in the dog. Vet Radiol 31 59-64, 1990
8. Vullo T, Korenman E, Manzo RP, et al: Diagnosis of cerebral ventriculomegaly in normal adult beagles using quantitative MRI. Vet Radiol Ultrasound 38:277-281, 1997
9. De Haan CE, Kraft SL, Gavin PR, et al: Normal variation in size of the lateral ventricles of the labrador retriever dog as assessed by magnetic resonance imaging. Vet Radiol 35:83-86, 1994
10. Kii S, Uzuka Y, Taura Y, et al: Developmental change of lateral ventricle volume and ratio in beagle-type dogs up to 7 months of age. Vet Radiol Ultrasound 39:185-189, 1998
11. Drake JM, Potts DG, Lemaire C: Magnetic resonance imaging of Silastic-induced canine hydrocephalus. Surg Neurol 31:28-40, 1989
12. Nishikawa M, Sakamoto H, Hakuba A, et al: Pathogenesis of Chiari malformation: a morphometric study of the posterior cranial fossa. J Neurosurg 86.40-47, 1997
13. Oldfield EH, Muraszko K, Shawker TH, et al. Pathophysiology of syringomyelia associated with Chiari I malformation of the cerebellar tonsils J Neurosurg 80:3-15, 1994
14. Kirberger RM, Jacobson LS, Davies JV, et al: Hydromyelia in the dog. Vet Radiol Ultrasound 38:30-38, 1997
15. Bagley RS, Harrington ML, Tucker RL, et al. Occipital dysplasia and associated cranial spinal cord abnormalities in two dogs. Vet Radiol Ultrasound 37:359-362, 1996
16. Truwit CL, Barkovich AJ: Disorders of brain development, in Atlas SW (ed): Magnetic Resonance Imaging of the Brain and Spine (2nd ed). Philadelphia, PA, Lippincott-Raven, 1996, pp 179-264
17. Byrd SE, Naidich TP: Common congenital brain abnormalities. Radiol Clin North Am 26:755-772, 1988
18. Pass DA, Howell JM, Thompson RR: Cerebellar malformation in two dogs and a sheep Vet Pathol 18:405-407, 1998
19. Kornegay JN: Cerebellar vermian hypoplasia in dogs. Vet Pathol 23:374-379, 1986
20. Schmid V, Lang J, Wolf M: Dandy-Walker—like syndrome in four dogs: cisternography as a diagnostic aid. J Am Anim Hosp Assoc 28:355-360, 1992
21. Regnier AM, Ducos de Lahitte MJ, Delisle MB, et al: Dandy-Walker syndrome in a kitten. J Am Anim Hosp Assoc 29:514-518, 1993
22. Kornegay JN: Ataxia of the head and limbs: cerebellar disease in dogs and cats. Prog Vet Neurol 1.255-274, 1990
23. de Lahunta A: Comparative cerebellar disease in domestic animals. Comp Contin Educ Pract Vet 11:8-19, 1980
24. DiRocco C. Arachnoid cysts, in Youmans JR (ed): Neurological Surgery (3rd ed). Philadelphia, PA, Saunders, 1990, pp 1299-1325
25. Milner RJ, Engela J, Kirberger RM: Arachnoid cyst in the cerebellar pontine area of a cat—diagnosis by magnetic resonance imaging. Vet Radiol Ultrasound 37:34-36, 1996
26. Vernau KM, Kortz GD, Koblik P, et al: Magnetic resonance imaging and computed tomography characteristics of intracranial intraarachnoid cysts in 6 dogs. Vet Radiol Ultrasound 38:171-176, 1997
27. Castel JP, Kissel P: Spontaneous intracerebral and infratentorial hemorrhage, in Youmans JR (ed): Neurological Surgery (3rd ed). Philadelphia, PA, Saunders, 1990, pp 1890-1917
28. Dukes J: Hypertension: a review of the mechanisms, manifestations, and management J Small Anim Pract 33:119-129, 1992
29. Fankhauser R, Luginbuhl H, McGrath JT: Cerebrovascular disease in various animal species. Ann N Y Acad Sci 127:817-859, 1965
30. Shores A, Cooper TG, Gartrell CL, et al: Clinical characteristics of cerebrovascular disease in small animals. Proc 9th ACVIM Forum 777-778, 1991
31. Thomas WB, Scheuler RO, Kornegay JN: Surgical excision of a cerebral arteriovenous malformation in a dog. Prog Vet Neurol 6:20-23, 1995
32. Hause WR, Helphrey ML, Green RW, et al: Cerebral arteriovenous malformation in a dog J Am Anim Hosp Assoc 18:601-607, 1982

33. Joseph RJ, Greenlee PG, Carrillo JM, et al: Canine cerebrovascular disease: clinical and pathological findings in 17 cases. J Am Anim Hosp Assoc 24:569-576, 1988
34. Bagley RS, Anderson WI, de Lahunta A, et al: Cerebellar infarction caused by arterial thrombosis in a dog. J Am Vet Med Assoc 192:785-787, 1988
35. Norton F: Cerebral infarction in a dog. Prog Vet Neurol 3 120-125, 1992
36. Tidwell AS, Mahony OM, Moore RP, et al: Computed tomography of an acute hemorrhagic cerebral infarct in a dog Vet Radiol Ultrasound 35:290-296, 1994
37. Thomas WB, Adams WH, McGavin MD, et al: Magnetic resonance imaging appearance of intracranial hemorrhage secondary to cerebral vascular malformation in a dog. Vet Radiol Ultrasound 38:371-375, 1997
38. Thomas WB, Sorjonen DC, Scheuler RO, et al: Magnetic resonance imaging of brain infarction in seven dogs. Vet Radiol Ultrasound 37:345-350, 1996
39. Stoffregen DA, Kallfelz FA, de Lahunta A: Cerebral hemorrhage in an old dog J Am Anim Hosp Assoc 21:495-498, 1985
40. Grossman RI. Intracranial hemorrhage, in Latchaw RE (ed): MR and CT Imaging of the Head, Neck, and Spine (2nd ed). St. Louis, MO, Mosby Year Book, 1991, pp 171-202
41. Enzman DR, Britt RH, Lyons BE, et al: Natural history of experimental intracerebral hemorrhage. sonography, computed tomography and neuropathology. Am J Neuroradiol 2:517-526, 1981
42. Wolf M, Pedroia V, Higgins RJ, et al: Intracranial ring enhancing lesions in dogs: a correlative CT scanning and neuropathologic study Vet Radiol Ultrasound 36.16-20, 1995
43. Thulborn KR, Atlas SW: Intracranial hemorrhage, in Atlas SW (ed): Magnetic Resonance Imaging of the Brain and Spine (2nd ed) Philadelphia, PA, Lippincott-Raven, 1996, pp 265-314
44. Thulborn KR, Brady TJ: Biochemical basis of the MR appearance of cerebral hemorrhage, in Edelman RR, Hesselink JR (eds). Clinical Magnetic Resonance Imaging. Philadelphia, PA, Saunders, 1990, pp 255-268
45. Brooks RA, Di Chiro G, Patronas N. MR imaging of cerebral hematomas at different field strengths: theory and applications. J Comput Assist Tomogr 13:194-206, 1989
46. Barkovich AJ, Atlas SW. Magnetic resonance imaging of intracranial hemorrhage. Radiol Clin North Am 26:801-820, 1988
47. Weingarten K. Zimmerman RD, Deo-Narine V. et al. MR imaging of acute intracranial hemorrhage: findings on sequential spin-echo and gradient-echo images in a dog model. Am J Neuroradiol 12:457-467, 1991
48. McCormick WF: Pathology of vascular malformations of the brain, in Wilson CB, Stein BM (eds): Intracranial Arteriovenous Malformations Baltimore, MD, Williams and Wilkins, 1984, pp 44-63
49. Mullan S, Mojtahedi S, Johnson DL, et al Embryological basis of some aspects of cerebral vascular fistulas and malformations J Neurosurg 85:1-8, 1996
50. Stein BM, Solomon RA. Arteriovenous malformations of the brain, in Youmans JR (ed): Neurological Surgery (3rd ed). Philadelphia, PA, Sunders, 1990, pp 1831-1863
51. Tarr RW, Hecht ST, Horton JA: Nontraumatic intracranial hemorrhage, in Latchaw RE (ed). MR and CT Imaging of the Head, Neck, and Spine (2nd ed). St. Louis, MO, Mosby Year Book 1991, pp 267-299
52. Atlas SW, Hurst RW: Intracranial vascular malformations and aneurysms, in Atlas SW (ed): Magnetic Resonance Imaging of the Brain and Spine (2nd ed) Philadelphia, PA, Lippincott-Raven, 1996, pp 489-556
53. Rigamonti D Drayer BP, Johnson PC, et al: The MRI appearance of cavernous malformations (angiomas) J Neurosurg 67:518-524, 1987
54. Kucharczyk W, Lemme-Pleghos L, Uske A, et al. Intracranial vascular malformations: MR and CT imaging. Radiology 156:383-389, 1985
55. Swayne DE, Tyler DE, Batker J: Cerebral infarction with associated venous thrombosis in a dog Vet Pathol 25:317-320, 1988
56. Toole JF, Burrow DD: Pathophysiology and clinical evaluation of ischemic vascular disease, in Youmans JR (ed): Neurological Surgery (3rd ed). Philadelphia, PA, Saunders, 1990, pp 1463-1515
57. Liu S, Tilley LP, Tappe JP, et al: Clinical and pathologic findings in dogs with atherosclerosis: 21 cases (1970-1983) J Am Vet Med Assoc 189.227-232, 1986
58. Zeiss CJ, Waddle G: Hypothyroidism and atherosclerosis in dogs. Comp Contin Educ Pract Vet 17.1117-1128, 1995
59. Patterson JS, Rusley MS, Zachary JF: Neurologic manifestations of cerebrovascular atherosclerosis associated with primary hypothyroidism in a dog J Am Vet Med Assoc 186:499-503, 1985
60. Cachin M, Vandevelde M: Cerebral infarction associated with thromboemboli. Proc 8th ACVIM Forum 1136-1136, 1990
61. Patton CS, Garner FM: Cerebral infarction caused by heartworms (*Dirofilaria immitis*) in a dog. J Am Vet Med Assoc 156:600-605, 1970
62. Hecht ST, Eelkema EA, Latchaw RE Cerebral ischemia and infarction, in Latchaw RE (ed). MR and CT Imaging of the Head and Neck. St. Louis, MO, Mosby Year Book, 1991, pp 145-169
63. Inoue Y Takemoto K, Miyamoto T, et al: Sequential computed tomography scans in acute cerebral infarction. Radiology 135:655-662, 1980
64. Brant-Zawadzki M, Periera B, Weinstein P, et al: MR imaging of acute experimental ischemia in cats. Am J Neuroradiol 7.7-11, 1986
65. Shuaib A, Lee D Pelz D, et al: The impact of magnetic resonance imaging on the management of acute ischemic stroke Neurology 42:816-818, 1992
66. Mathews VP, Whitlow WD, Bryan RN: Cerebral ischemia and infarction, in Atlas SW (ed). Magnetic Resonance Imaging and the Brain (2nd ed). Philadelphia, PA, Lippincott-Raven, 1996, pp 557-609
67. Imakita S, Nishimura T, Naito H, et al: Magnetic resonance imaging of human cerebral infarction: enhancement with Gd-DTPA. Neuroradiology 29:422-429, 1987
68. Drayer BP, Muraki A, Osborne D, et al: Gd-DTPA–enhanced magnetic resonance imaging for study of blood-brain–barrier permeability in naturally occurring and experimentally induced brain infarction, in Runge VM, Clausen C, Felix R, et al (eds): Contrast Agents in Magnetic Resonance Imaging. Amsterdam, Excerpta Medica, 1986, pp 114-117
69. Jacobs BC, Brant-Zawadzki M: Ischemia, in Stark DD, Bradley WG (eds): Magnetic Resonance Imaging. St Louis, MO, Mosby Year Book, 1992, pp 636-669
70. Montgomery DL, Lee AC: Brain damage in the epileptic beagle dog Vet Pathol 20:160-169, 1983
71. Lothman EL: The biochemical basis and pathophysiology of status epilepticus. Neurology 40 13-23, 1990 (suppl 2)
72. VanLandingham KE, Heinz ER, Cavazos JE, et al: Magnetic resonance imaging evidence of hippocampal injury after prolonged focal febrile convulsions. Ann Neurol 43:413-426, 1998
73. Aykut-Bingol C, Tekin S, Ince D, et al: Reversible MRI lesions after seizures. Seizure 6:237-239, 1997
74. Mellema LM, Koblik PD, Kortz GD, et al: Reversible magnetic resonance imaging abnormalities in dogs following seizures. Vet Radiol Ultrasound 39:583, 1998 (abstr)
75. Gentry LR: Imaging of closed head injury. Radiology 191 1-17, 1994
76. Gentry LR: Head trauma, in Atlas SW (ed): Magnetic Resonance Imaging of the Brain and Spine (2nd ed). Philadelphia, PA, Lippincott-Raven, 1998, pp 611-648
77. Orrison WW, Gentry LR, Stimac GK, et al: Blinded comparison of cranial CT and MR in closed head injury evaluation. Am J Neuroradiol 15 351-356, 1994
78. Eelkema EA, Hecht ST, Horton JA: Head trauma, in Latchaw RE (ed): MR and CT Imaging of the Head, Neck, and Spine (2nd ed). St. Louis, MO, Mosby Year Book, 1991, pp 203-265
79. Gennarelli TA: Mechanisms of brain injury J Emerg Med 11:5-11, 1993
80. Mittl RL, Grossman RI, Hiehle JF, et al: Prevalence of MR evidence of diffuse axonal injury in patients with mild head injury and normal head CT findings. Am J Neuroradiol 15.1583-1589, 1994
81. Jungreis CA, Grossman RI: Intracranial infectious and inflammatory diseases, in Latchaw RE (ed). MR and CT Imaging of the Head, Neck, and Spine (2nd ed). St Louis, MO, Mosby, 1991, pp 303-346
82. Thomas WB: Inflammatory diseases of the central nervous system in dogs. Clin Tech Small Anim Pract 13.167-178, 1998
83. Tipold A, Jaggy A: Steroid responsive meningitis-arteritis in dogs: Long term study of 32 cases. J Small Anim Pract 35:311-316, 1994

84. Meric SM Canine meningitis: a changing emphasis. J Vet Int Med 2:26-35, 1988
85. Quagliarello V, Scheld WM: Bacterial meningitis· pathogenesis, pathophysiology, and progress. N Engl J Med 327:864-872, 1992
86. Lowrie CT, Kumar K, Moore JB, et al: A preliminary study of magnetic resonance imaging (MRI) in experimental canine meningitis. Companion Anim Pract 19 3-6, 1989
87. Mathews VP, Kuharik MA, D'Amour PG, et al: Gd-DTPA-enhanced MR imaging of experimental bacterial meningitis; evaluation and comparison with CT. Am J Roentgenol 152:131-136, 1989
88. Barnes PD, Poussaint TY, Burrows PE Imaging of pediatric central nervous system infections. Neuroimaging Clin North Am 4:367-391 1994
89. Whiteman MLH, Bowen BC, Post MJD, et al: Intracranial infection, in Atlas SW (ed): Magnetic Resonance Imaging of the Brain and Spine (2nd ed) Philadelphia, PA, Lippincott-Raven, 1996, pp 707-772
90. Thomas WB, Sorjonen DC, Steiss JE: A retrospective evaluation of 38 cases of canine distemper encephalomyelitis. J Am Anim Hosp Assoc 29:23-28, 1993
91. Tipold A, Vandevelde M, Jaggy A. Neurological manifestations of canine distemper infection. J Small Anim Pract 33:466-470, 1992
92. Tipold A: Diagnosis of inflammatory and infectious diseases of the central nervous system in dogs: a retrospective study. J Vet Int Med 9:304-314, 1995
93. Plummer SB, Wheeler SJ, Thrall DE, et al: Computed tomography of primary inflammatory brain disorders in dogs and cats. Vet Radiol 33:307-372, 1992
94. Thomson CE, Kornegay JN, Burn RA, et al: Magnetic resonance imaging—a general overview of principles and examples in veterinary neurodiagnosis Vet Radiol Ultrasound 34:2-17, 1993
95. Kline KL, Joseph RJ, Averill DA Feline infectious peritonitis with neurologic involvement: clinical and pathological findings in 24 cats. J Am Anim Hosp Assoc 30:111-118, 1994
96. Baroni M, Heinold Y: A review of the clinical diagnosis of feline infectious peritonitis viral meningoencephalomyelitis. Prog Vet Neurol 6:88-94, 1995
97. Foley JE, Lapointe J-M, Koblik P, et al: Diagnostic features of clinical neurologic feline infectious peritonitis. J Vet Int Med 12:415-423, 1998
98. Summers BA, Cummings JF, de Lahunta A: Inflammatory diseases of the central nervous system, in Veterinary Neuropathology. St. Louis, MO, Mosby, 1995, pp 95-188
99. Thomas WB: What is your diagnosis? (feline infectious virus encephalitis). Prog Vet Neurol 6 35-37, 1995
100. Berthelin CF, Bailey CS, Kass PH, et al: Cryptococcosis of the nervous system in dogs, Part 1: Epidemiologic, clinical, and neuropathologic features. Prog Vet Neurol 5·88-97, 1994
101. Gerds-Grogan S, Dayrell-Hart B: Feline cryptococcosis: a retrospective evaluation. J Am Anim Hosp Assoc 33:118-122, 1997
102. Glass E, deLahunta A, Kent M, et al: A cryptococcal granuloma in the brain of a cat causing focal signs Prog Vet Neurol 7.141-144, 1996
103. Tiches D, Vite CH, Dayrell-Hart B, et al. A case of canine central nervous system cryptococcosis: management with fluconazole. J Am Anim Hosp Assoc 34:145-151, 1998
104. Arceneaux KA, Taboada J, Hosgood G: Blastomycosis in dogs 115 cases (1980-1995). J Am Vet Med Assoc 213:658-664, 1998
105. Breider MA, Walker TL, Legendre AM, et al: Blastomycosis in cats: five cases (1979-1986). J Am Vet Med Assoc 193:570-572, 1988
106. Schaer M, Johnson KE, Nicholson AC: Central nervous system disease due to histoplasmosis in a dog: a case report J Am Anim Hosp Assoc 19:311-316, 1983
107. Burk RL, Joseph R, Baer K: Systemic aspergillosis in a cat Vet Radiol 31:26-28, 1990
108. Pryor WH, Huizenga CG, Splitter GA, et al: *Coccidioides immitis* encephalitis in two dogs. J Am Vet Med Assoc 161:1108-1112, 1972
109. Burtch M: Granulomatous meningitis caused by *Coccidioides immitis* in a dog. J Am Vet Med Assoc 212:827-829, 1998
110. Migaki G, Casey HW, Bayles WB Cerebral phaeohyphomycosis. J Am Vet Med Assoc 191:997-998, 1987
111. Fiske RE, Choyce PD, Whitford HW: Phaeohyphomycotic encephalitis in two dogs. J Am Anim Hosp Assoc 22:327-330, 1985
112. Cordy DR, Holliday TA: A necrotizing meningoencephalitis of pug dogs. Vet Pathol 26 191-194, 1989
113. Tipold A, Fatzer R, Jaggy A, et al: Necrotizing encephalitis in Yorkshire terriers. J Small Anim Pract 34:623-628, 1993
114. Stalis IH, Chadwick B, Dayrell-Hart B, et al: Necrotizing meningoencephalitis of Maltese dogs. Vet Pathol 32:230-235, 1995
115. Jull BA, Merryman JI, Thomas WB, et al: Necrotizing encephalitis in a Yorkshire terrier. J Am Vet Med Assoc 211:1005-1007, 1997
116. Sawashima Y, Sawashima K, Taura Y, et al: Clinical and pathological findings of a Yorkshire terrier affected with necrotizing encephalitis. J Vet Med Sci 58 659-661, 1996
117. Braund KG, Vandevelde M, Walker TL, et al· Granulomatous meningoencephalomyelitis in six dogs. J Am Vet Med Assoc 172.1195-1200, 1978
118. Sorjonen DC: Clinical and histopathological features of granulomatous meningoencephalomyelitis in dogs. J Am Anim Hosp Assoc 26:141-147, 1990
119. Cordy DR Canine granulomatous meningoencephalomyelitis. Vet Pathol 16 325-333, 1979
120. Alley MR, Jones BR, Johnstone AC: Granulomatous meningoencephalomyelitis of dogs in New Zealand. N Z Vet J 37:117-119, 1983
121. Thomas JB, Eger C: Granulomatous meningoencephalomyelitis in 21 dogs. J Small Anim Pract 30 287-293, 1989
122. Sarfaty D, Carrillo JM, Greenlee PG. Differential diagnosis of granulomatous meningoencephalitis, distemper, and suppurative meningoencephalitis in the dog. J Am Vet Med Assoc 188:387-392, 1986
123. Munana KR, Luttgen PJ Prognostic factors for dogs with granulomatous meningoencephalomyelitis: 42 cases (1982-1996). J Am Vet Med Assoc 212.1902-1906, 1998
124. Dzyban LA, Tidwell AS Imaging diagnosis—granulomatous meningoencephalitis in a dog. Vet Radiol Ultrasound 37:428-430, 1996
125. Speciale J, Van Winkle TJ, Steinberg SA, et al Computed tomography in the diagnosis of focal granulomatous meningoencephalitis: retrospective evaluation of three cases. J Am Anim Hosp Assoc 28:327-332, 1992
126. Lobetti RG, Pearson J: Magnetic resonance imaging in the diagnosis of focal granulomatous meningoencephalitis in two dogs. Vet Radiol Ultrasound 37:424-427, 1996
127. McCandlish IAP, Ormerod EJ: Brain abscess associated with a penetrating foreign body. Vet Record 102:380-381, 1978
128. Heavner JEPM: Brain abscess in a dog. Veterinary Medicine/Small Animal Clinician 71 785-793, 1976
129. Britt RH, Enzman DR, Yeager AS: Neuropathological and computerized tomographic findings in experimental brain abscess J Neurosurg 55:590-603, 1981
130. Enzman DR, Britt RH, Yeager AS: Experimental brain abscess; computed tomographic and neuropathologic correlation. Radiology 133:113-122, 1979
131. Enzman DR, Britt RH, Placone R: Staging of human brain abscess by computed tomography. Radiology 146:703-708, 1983
132. Sze G, Zimmerman RD: The magnetic resonance imaging of infections and inflammatory diseases. Radiol Clin North Am 26:839-849, 1988
133. Sartin EA, Hendrix CM, Dillehay DL, et al: Cerebral cuterebrosis in a dog. J Am Vet Med Assoc 189:1338-1339, 1986
134. Hendrix CM, Cox NR, Clemons-Chervis C, et al: Aberrant intracranial myiasis caused by larval *Cuterebra* infection. Comp Contin Educ Pract Vet 11 550-559, 1989
135. Glass EN Cornetta AM, deLahunta A, et al: Clinical and clinicopathologic features in 11 cats with Cuterebra larvae myiasis of the central nervous system. J Vet Int Med 12:365-368, 1998
136. Smith MC, Bailey CS, Baker N, et al: Cerebral coenurosis in a cat. J Am Vet Med Assoc 192:82-84, 1988
137. Slocombe RF, Arundel JH, Labuc R et al: Cerebral coenuriasis in a domestic cat Austral Vet J 66:92-93, 1998
138. Bradley WG Hemorrhage and brain iron, in Stark DD, WG Bradley (eds): Magnetic Resonance Imaging (2nd ed). St Louis, MO, Mosby Year Book, 1992, pp 721-769
139. Thomas WB: Cerebrovascular disease. Vet Clin North Am Small Anim Pract 26:925-943, 1996